

TABM: ADVANCING TABULAR DEEP LEARNING WITH PARAMETER-EFFICIENT ENSEMBLING

Yury Gorishniy *
Yandex

Akim Kotelnikov
HSE University, Yandex

Artem Babenko
Yandex

ABSTRACT

Deep learning architectures for supervised learning on tabular data range from simple multilayer perceptrons (MLP) to sophisticated Transformers and retrieval-augmented methods. This study highlights a major, yet so far overlooked opportunity for substantially improving tabular MLPs: namely, parameter-efficient ensembling — a paradigm for implementing an ensemble of models as one model producing multiple predictions. We start by developing TabM — a simple model based on MLP and our variations of BatchEnsemble (an existing technique). Then, we perform a large-scale evaluation of tabular DL architectures on public benchmarks in terms of both task performance and efficiency, which renders the landscape of tabular DL in a new light. Generally, we show that MLPs, including TabM, form a line of stronger and more practical models compared to attention- and retrieval-based architectures. In particular, we find that TabM demonstrates the best performance among tabular DL models. Lastly, we conduct an empirical analysis on the ensemble-like nature of TabM. For example, we observe that the multiple predictions of TabM are weak individually, but powerful collectively. Overall, our work brings an impactful technique to tabular DL, analyses its behaviour, and advances the performance-efficiency trade-off with TabM — a simple and powerful baseline for researchers and practitioners. The code is available at: <https://github.com/yandex-research/tabm>.

1 INTRODUCTION

Supervised learning on tabular data is a ubiquitous machine learning (ML) scenario in a wide range of industrial applications. Among classic non-deep-learning methods, the state-of-the-art solution for such tasks is gradient-boosted decision trees (GBDT) (Prokhorenkova et al., 2018; Chen & Guestrin, 2016; Ke et al., 2017). Deep learning (DL) models for tabular data, in turn, are reportedly improving, and the most recent works claim to perform on par or even outperform GBDT on academic benchmarks (Hollmann et al., 2023; Chen et al., 2023b;a; Gorishniy et al., 2024).

However, from the practical perspective, it is unclear if tabular DL offers any obvious go-to baselines beyond simple architectures in the spirit of a multilayer perceptron (MLP). *First*, the scale and consistency of performance improvements of new methods w.r.t. simple MLP-like baselines are not always explicitly analyzed in the literature. Thus, one has to infer those statistics from numerous per-dataset performance scores, which makes it hard to reason about the progress. At the same time, due to the extreme diversity of tabular datasets, consistency is an especially valuable and hard-to-achieve property for a hypothetical go-to baseline. *Second*, efficiency-related properties, such as training time, and especially inference throughput, sometimes receive less attention. While methods are usually equally affordable on small-to-medium datasets (e.g. <100K objects), their applicability to larger datasets remains uncertain. *Third*, some recent work generally suggests that the progress on academic benchmarks may not transfer that well to real-world tasks (Rubachev et al., 2024). With all the above in mind, in this work, we thoroughly evaluate existing tabular DL methods and find that non-MLP models do not yet offer a convincing replacement for MLPs.

At the same time, we identify a previously overlooked path towards more powerful, reliable and reasonably efficient tabular DL models. In a nutshell, we find that the parameter-efficient approach to

*The corresponding author: yurygorishniy@gmail.com

deep ensembling, where most weights are shared between ensemble members, allows making simple and strong tabular models out of plain MLPs. For example, MLP coupled with BatchEnsemble (Wen et al., 2020) — a long-existing method — right away outperforms popular attention-based models, such as FT-Transformer (Gorishniy et al., 2021), while being simpler and more efficient. This result alone suggests that the parameter-efficient ensembling is a low-hanging fruit for tabular DL.

Our work builds on the above observations, and offers TabM — a new powerful and practical model for researchers and practitioners. Drawing an informal parallel with GBDT (an ensemble of decision trees), TabM can also be viewed as a simple base model (MLP) combined with an ensembling-like technique, providing high performance and simple implementation at the same time.

Main contributions. We summarize our main contributions as follows:

1. We present TabM — a simple DL architecture for supervised learning on tabular data. TabM is based on MLP and parameter-efficient ensembling techniques closely related to BatchEnsemble (Wen et al., 2020). In particular, TabM produces Multiple predictions per object. TabM easily competes with GBDT and outperforms prior tabular DL models, while being more efficient than attention- and retrieval-based DL architectures.
2. We provide a fresh perspective on tabular DL models in a large-scale evaluation along four dimensions: performance ranks, performance score distributions, training time and inference throughput. One of our findings is that MLPs, including TabM, hit an appealing performance-efficiency tradeoff, which is not the case for attention- and retrieval-based models.
3. Empirically, we show that the multiple predictions of TabM are weak and overfitted individually, while their average is strong and generalizable. The training gradients of TabM, in turn, can be viewed as an “ensemble” of diverse gradients coming from the multiple predictions.

2 RELATED WORK

Decision-tree-based models. Gradient-boosted decision trees (GBDT) (Chen & Guestrin, 2016; Ke et al., 2017; Prokhorenkova et al., 2018) is a strong and efficient baseline for tabular tasks. GBDT is a classic machine learning model, specifically, an ensemble of decision trees. Our model TabM is a deep learning model, specifically, a parameter-efficient ensemble of MLPs.

Tabular deep learning architectures. A large number of deep learning architectures for tabular data has been proposed over the recent years. That includes attention-based architectures (Song et al., 2019; Gorishniy et al., 2021; Somepalli et al., 2021; Kossen et al., 2021; Yan et al., 2023), retrieval-augmented architectures (Somepalli et al., 2021; Kossen et al., 2021; Gorishniy et al., 2024; Ye et al., 2024), MLP-like models (Gorishniy et al., 2021; Klambauer et al., 2017; Wang et al., 2020) and others (Arik & Pfister, 2020; Popov et al., 2020; Chen et al., 2023b; Marton et al., 2024; Hollmann et al., 2023). Compared to prior work, the key difference of our model TabM is its computation flow, where one TabM imitates an ensemble of MLPs by producing multiple independently trained predictions. Prior attempts to bring ensemble-like elements to tabular DL (Badirli et al., 2020; Popov et al., 2020) were not found promising (Gorishniy et al., 2021). Also, being a simple feed-forward MLP-based model, TabM is significantly more efficient than some of the prior work. Compared to attention-based models, TabM does not suffer from quadratic computational complexity w.r.t. the dataset dimensions. Compared to retrieval-based models, TabM is easily applicable to large datasets.

Improving tabular MLP-like models. Multiple recent studies achieved competitive performance with MLP-like architectures on tabular tasks by applying architectural modifications (Gorishniy et al., 2022), regularizations (Kadra et al., 2021; Jeffares et al., 2023a; Holzmüller et al., 2024), custom training techniques (Bahri et al., 2021; Rubachev et al., 2022). Thus, it seems that tabular MLPs have good potential, but one has to deal with overfitting and optimization issues to reveal that potential. Our model TabM achieves high performance with MLP in a different way, namely, by using it as the base backbone in a parameter-efficient ensemble in the spirit of BatchEnsemble (Wen et al., 2020). Our approach is orthogonal to the aforementioned training techniques and architectural advances.

Deep ensembles. In this paper, by a deep ensemble, we imply multiple DL models of the same architecture trained independently (Jeffares et al., 2023b) for the same task under different random seeds (i.e. with different initializations, training batch sequences, etc.). The prediction of a deep ensemble is the mean prediction of its members. Deep ensembles often significantly outperform single DL models of the same architecture (Fort et al., 2020), and can excel in other tasks like uncertainty

estimation or out-of-distribution detection (Lakshminarayanan et al., 2017). It was observed that individual members of deep ensembles can learn to extract diverse information from the input, and the power of deep ensembles depends on this diversity (Allen-Zhu & Li, 2023). The main drawback of deep ensembles is the cost and inconvenience of training and using multiple models.

Parameter-efficient deep “ensembles”. To achieve the performance of deep ensembles at a lower cost, multiple studies proposed architectures that imitate ensembles by producing multiple predictions with one model (Lee et al., 2015; Zhang et al., 2020; Wen et al., 2020; Havasi et al., 2021; Antorán et al., 2020; Turkoglu et al., 2022). Such models can be viewed as “ensembles” where the implicit ensemble members share a large amount of their weights. There are also non-architectural approaches to efficient ensembling, e.g. FGE (Garipov et al., 2018), but we do not explore them, because we are interested specifically in architectural techniques. In this paper, we highlight parameter-efficient ensembling as an impactful paradigm for tabular DL. In particular, we describe two simple variations of BatchEnsemble (Wen et al., 2020) that are highly effective for tabular MLPs. One variation uses a more efficient parametrization, and another one uses an improved initialization.

3 TABM

In this section, we present TabM — a **T**abular DL model that makes **M**ultiple predictions.

3.1 PRELIMINARIES

Notation. We consider classification and regression tasks on tabular data. x and y denote the features and a label, respectively, of one object from a given dataset. A machine learning model takes x as input and produces \hat{y} as a prediction of y . $N \in \mathbb{N}$ and $d \in \mathbb{N}$ respectively denote the “depth” (e.g. the number of blocks) and “width” (e.g. the size of the latent representation) of a given neural network. $d_y \in \mathbb{N}$ is the output representation size (e.g. $d_y = 1$ for regression tasks, and d_y equals the number of classes for classification tasks).

Datasets. Our benchmark consists of 46 publicly available datasets used in prior work, including Grinsztajn et al. (2022); Gorishniy et al. (2024); Rubachev et al. (2024). The main properties of our benchmark are summarized in Table 1, and more details are provided in Appendix C.

Table 1: The overview of our benchmark. The “Split type” property is explained in the text.

#Datasets	Train size				#Features				Task type		Split type	
	Min.	Q50	Mean	Max.	Min.	Q50	Mean	Max.	#Regr.	#Classif.	Random	Domain-aware
46	1.8K	12K	76K	723K	3	20	108	986	28	18	37	9

Domain-aware splits. We pay extra attention to datasets with what we call “domain-aware” splits, including the eight datasets from Rubachev et al. (2024) and the Microsoft dataset (Qin & Liu, 2013). For these datasets, their original real-world splits are available, for example, time-aware splits as in Rubachev et al. (2024). Such datasets were shown to be challenging for some methods, because they naturally exhibit a certain degree of distribution shift between training and test parts (Rubachev et al., 2024). The random splits of the remaining 37 datasets are inherited from prior work.

Experiment setup. We use the setup from Gorishniy et al. (2024), and describe it in detail in subsection D.2. Most importantly, on each dataset, a given model undergoes hyperparameter tuning on the *validation* set, then the tuned model is trained from scratch under multiple random seeds, and the *test* metric averaged over the random seeds becomes the final score of the model on the dataset.

Metrics. We use RMSE (the root mean square error) for regression tasks, and accuracy or ROC-AUC for classification tasks depending on the dataset source. See subsection D.3 for details.

Also, throughout the paper, we often use the relative performance of models w.r.t. MLP as the key metric. This metric gives a unified perspective on all tasks and allows reasoning about the scale of improvements w.r.t. to a simple baseline (MLP). Formally, on a given dataset, the metric is defined as $\left(\frac{\text{score}}{\text{baseline}} - 1\right) \cdot 100\%$, where “score” is the metric of a given model, and “baseline” is the metric of MLP. In this computation, for regression tasks, we convert the raw metrics from RMSE to R^2 to better align the scales of classification and regression metrics.

3.2 A QUICK INTRODUCTION TO BATCHEMSEMBLE.

For a given architecture, let's consider any linear layer l in it: $l(x) = Wx + b$, where $x \in \mathbb{R}^{d_1}$, $W \in \mathbb{R}^{d_2 \times d_1}$, $b \in \mathbb{R}^{d_2}$. To simplify the notation, let $d_1 = d_2 = d$. In a traditional deep ensemble, the i -th member has its own set of weights W_i, b_i for this linear layer: $l_i(x_i) = W_i x_i + b_i$, where x_i is the object representation within the i -th member. By contrast, in BatchEnsemble, this linear layer is either (1) fully shared between all members, or (2) mostly shared: $l_i(x_i) = s_i \odot (W(r_i \odot x_i)) + b_i$, where \odot is the elementwise multiplication, $W \in \mathbb{R}^{d \times d}$ is shared between all members, and $r_i, s_i, b_i \in \mathbb{R}^d$ are *not* shared between the members. This is equivalent to defining the i -th weight matrix as $W_i = W \odot (r_i s_i^T)$. To ensure diversity of the ensemble members, r_i and s_i of all members are initialized randomly with ± 1 . All other layers are fully shared between the members of BatchEnsemble.

The described parametrization allows packing all ensemble members in one model that simultaneously takes k copies of the object as input, and applies all k implicit members in parallel, without explicitly materializing each member. This is achieved by replacing one or more linear layers of the original neural network with their BatchEnsemble versions: $l_{BE}(X) = ((X \odot R)W) \odot S + B$, where $X \in \mathbb{R}^{k \times d}$ stores k representations of the same input object (one per member), and $R, S, B \in \mathbb{R}^d$ store the non-shared weights (r_i, s_i, b_i) of the members, as shown at the lower left part of [Figure 1](#).

Overhead to the model size. With BatchEnsemble, adding a new ensemble member means adding only one row to each of the matrices R, S and B , which results in $3d$ new parameters per layer. For typical values of d , this is a negligible overhead to the original layer size $d^2 + d$.

Overhead to the runtime. Thanks to the modern hardware, the large number of shared weights and the parallel execution of the k forward passes, the runtime overhead of BatchEnsemble can be (significantly) lower than $\times k$ ([Wen et al., 2020](#)). Intuitively, if the original workload underutilizes the hardware, there are more chances to pay less than $\times k$ overhead.

Terminology. In this paper, we call r_i, s_i, b_i, R, S and B *adapters*, and the implicit members of parameter-efficient ensembles (e.g. BatchEnsemble) — *implicit submodels* or simply *submodels*.

3.3 TABM_{mini} & TABM

Our models TabM_{mini} and TabM are based on a multilayer perceptron (MLP) and parameter-efficient ensembling methods, with a strong connection to BatchEnsemble ([Wen et al., 2020](#)), introduced in [subsection 3.2](#). In [subsection A.1](#), we explain that we use specifically BatchEnsemble as the baseline efficient ensembling method because of its good balance between performance and ease of use, while using MLP as the base model is crucial because of its excellent efficiency. We obtain our models in several steps, starting from essential baselines. We always use the ensemble size $k = 32$ and analyze this hyperparameter in [subsection 5.3](#).

MLP. We define MLP as a sequence of N simple blocks followed by a linear prediction head: $\text{MLP}(x) = \text{Linear}(\text{Block}_N(\dots(\text{Block}_1(x))))$, where $\text{Block}_i(x) = \text{Dropout}(\text{ReLU}(\text{Linear}(x)))$.

MLP $\times k$ = MLP + Deep Ensemble. We denote the traditional deep ensemble of k independently trained MLPs as MLP $\times k$. This method is illustrated in [Figure 1](#), and its performance is reported in [Figure 2](#) (the hyperparameter tuning is performed for one MLP, after which the tuned MLP is ensembled). Interestingly, the results are already better and more stable than those of FT-Transformer ([Gorishniy et al., 2021](#)) — the popular attention-based baseline. And, given the significantly better efficiency of MLPs (as will be shown later), MLP $\times k$ may actually be no less practical than FT-Transformer, especially with additional techniques like Packed-Ensembles ([Laurent et al., 2023](#)). That said, we continue towards more efficient approaches.

TabM_{naive} = MLP + BatchEnsemble. Now, instead of the deep ensemble, we naively apply BatchEnsemble to the backbone of MLP, while keeping the prediction heads separate. This gives us TabM_{naive} — a preliminary suboptimal version of TabM. In fact, the architecture (but not the initialization) of TabM_{naive} is already equivalent to that of TabM, so [Figure 1](#) is applicable. The performance of TabM_{naive} shown in [Figure 2](#) is important for two reasons. First, TabM_{naive} — the efficient version of MLP $\times k$ — is noticeably better than MLP $\times k$ itself, which is intriguing. We are not aware of similar results for BatchEnsemble in general, and share some thoughts on this phenomenon in [subsection A.2](#). Second, TabM_{naive} right away outperforms FT-Transformer, which demonstrates the great potential of parameter-efficient ensembling for MLPs. This motivates further exploration.

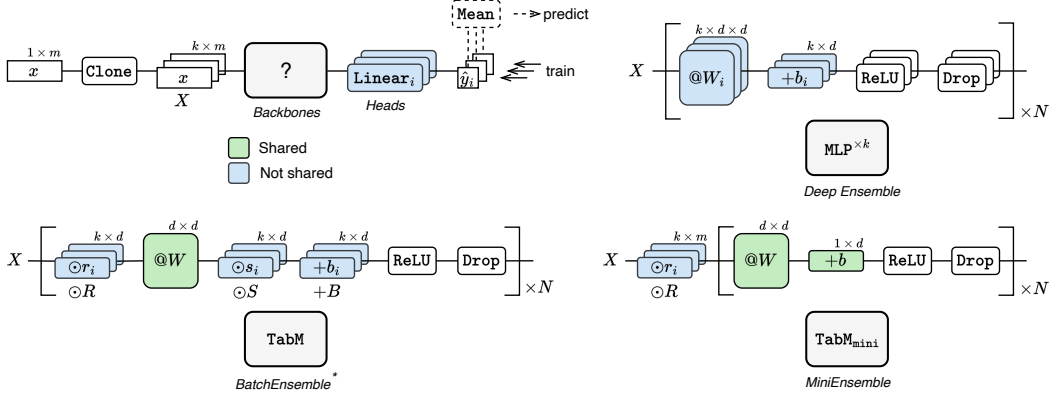


Figure 1: (Upper left) A template for implementing an ensemble of k MLPs. The remaining parts of the figure are three different parametrizations of the k MLP backbones, all described in [subsection 3.3](#). In all cases, each of the k MLP backbones independently processes its own copy of the input object. (Upper right) $\text{MLP}^{\times k}$ is a traditional deep ensemble of k fully independent MLPs. (Lower left) TabM is obtained by injecting three non-shared adapters R, S, B in each of the N linear layers of *one* MLP (* the initialization differs from [Wen et al. \(2020\)](#)). (Lower right) TabM_{mini} is obtained by keeping only the very first adapter R of TabM and removing the remaining $3N - 1$ adapters. Thus, TabM_{mini} applies the same shared MLP to k object representations, with only two non-shared elements ensuring diversity of predictions: the randomly initialized multiplicative adapter R and the k prediction heads. (Details) Input transformations such as one-hot-encoding, feature embeddings ([Gorishniy et al., 2022](#)) and others are omitted for simplicity. In practice, they are applied (and the result is flattened) before the Clone module. Drop denotes dropout ([Srivastava et al., 2014](#)).

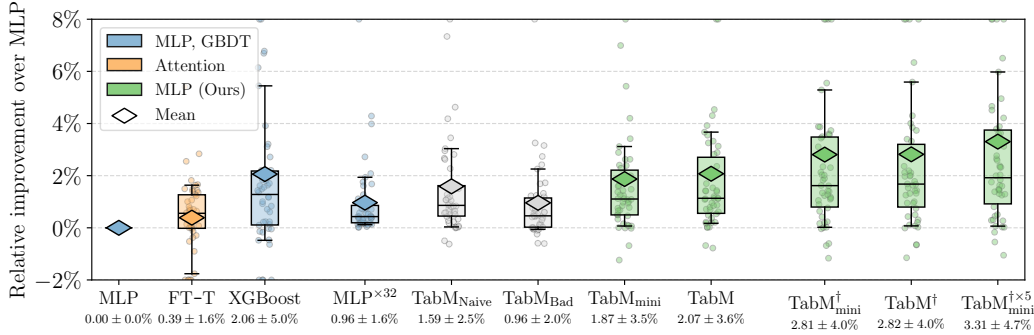


Figure 2: The performance of models described in [subsection 3.3](#) on 46 datasets from [Table 1](#); plus several baselines on the left. For a given model, one dot on a jitter plot describes the performance score on one of the 46 datasets. The box plots describe the percentiles of the jitter plots: the boxes describe the 25th, 50th and 75th percentiles, and the whiskers describe the 10th and 90th percentiles. Outliers are clipped. The numbers at the bottom are the mean and standard deviations over the jitter plots. For each model, hyperparameters are tuned. “Model^{×k}” denotes an ensemble of k models.

TabM_{mini} = MLP + MiniEnsemble. By construction, the just discussed TabM_{naive} (illustrated as “TabM” in [Figure 1](#)) has $3N$ adapters: R, S and B in each of the N blocks. Among the $3N$ adapters, the first adapter R in the very first linear layer is responsible for transforming the k equal copies of the input (packed as X in [Figure 1](#)) to k different representations *before* the tabular features are mixed with $@W$ for the first time. A simple experiment reveals that this adapter is critical. First, we remove it from TabM_{naive} and keep the remaining $3N - 1$ adapters untouched, which gives us TabM_{bad} with worse performance, as shown in [Figure 2](#). Then, we do the opposite: we keep only the very first adapter of TabM_{naive} and remove the remaining $3N - 1$ adapters, which gives us TabM_{mini} — the minimal version of TabM. TabM_{mini} is illustrated in [Figure 1](#), where we call the described approach “MiniEnsemble”. Perhaps, surprisingly, but [Figure 2](#) shows that TabM_{mini} performs better than TabM_{naive}, despite having only one adapter instead of $3N$ adapters.

TabM = MLP + BatchEnsemble + Better initialization. The just obtained results motivate the next step. We go back to the architecture of $\text{TabM}_{\text{naive}}$ with all $3N$ adapters, but initialize all multiplicative adapters R and S , except for the very first one, deterministically with 1. As such, at initialization, the deterministically initialized adapters have no effect, and the model behaves like $\text{TabM}_{\text{mini}}$, but these adapters are free to add more expressivity during training. This gives us TabM, illustrated in Figure 1. Figure 2 shows that TabM is the best variation so far.

$\text{TabM}_{\text{mini}}^\dagger$ & TabM^\dagger . Non-linear feature embeddings (Gorishniy et al., 2022) are known to boost the performance of many tabular models, especially of MLPs. We denote $\text{TabM}_{\text{mini}}$ and TabM with non-linear feature embeddings as $\text{TabM}_{\text{mini}}^\dagger$ and TabM^\dagger , respectively. By default, we recommend using the piecewise-linear embeddings (Gorishniy et al., 2022). In subsection A.3, we provide additional implementation details, such as slightly different initialization. Figure 2 shows that, $\text{TabM}_{\text{mini}}^\dagger$ is competitive with TabM^\dagger , so we will use $\text{TabM}_{\text{mini}}^\dagger$ for simplicity.

Intuition. To give additional intuition on TabM, we make the following observations:

- Setting $k = 1$ makes TabM identical to one plain MLP.
- Increasing k by one adds a negligible number of new parameters to TabM.
- TabM, viewed as a single model, can benefit from the deep ensembling, see $\text{TabM}_{\text{mini}}^{\dagger \times 5}$ in Figure 2.
- In Transformer-like (Vaswani et al., 2017) and Mixer-like (Tolstikhin et al., 2021) models:
 - (a) the latent representation shape is $m \times d$, where m is the number of tabular features, and d is the embedding size;
 - (b) the m embeddings are mixed with each other in attention or linear layers, and
 - (c) per-embedding transformations (the FFN layers) are the same for all embeddings.
 By contrast, in TabM: (a) the shape is only $k \times d$, (b) the k embeddings never interact with each other, and (c) per-embedding transformations contain embedding-specific weights (adapters).

Hyperparameters. Compared to MLP, the only new hyperparameter of TabM is k — the number of implicit submodels. We heuristically set $k = 32$ and do not tune this value. We analyze the influence of k in subsection 5.3. We also noticed that the average optimal learning rate for TabM is higher than for MLP, which is explained in subsection A.4.

Limitations and practical considerations are commented in subsection A.5.

Next steps. The performance of TabM in Figure 2 renders it as a highly promising model. This motivates a full-fledged empirical comparison against prior tabular models (section 4) and detailed analysis of TabM’s behaviour (section 5).

4 EVALUATING TABULAR DEEP LEARNING ARCHITECTURES

Now, we perform an empirical comparison of many tabular models, including TabM introduced in section 3. The implementation details of the models are provided in Appendix D.

4.1 BASELINES

In the main text, we use the following baselines: MLP (the classic multilayer perceptron), FT-Transformer denoted as “FT-T” (the attention-based model from Gorishniy et al. (2021)), SAINT (the attention- and retrieval- based model from Somepalli et al. (2021)), T2G-Former denoted as “T2G” (the attention-based model from Yan et al. (2023)), ExcelFormer denoted as “Excel” (the attention-based model from Chen et al. (2023a)), TabR (the retrieval-based model from Gorishniy et al. (2024)), ModernNCA denoted as “MNCA” (the retrieval-based model from Ye et al. (2024)) and three GBDT implementations: XGBoost (Chen & Guestrin, 2016), LightGBM (Ke et al., 2017) and CatBoost (Prokhorenkova et al., 2018).

The models with non-linear feature embeddings from Gorishniy et al. (2022) are marked with \dagger or \ddagger depending on the embedding type (see subsection D.8 for details on feature embeddings):

- MLP^\dagger and $\text{TabM}_{\text{mini}}^\dagger$ use a modified version of the piecewise-linear embeddings.
- TabR^\ddagger , MNCA^\ddagger , and MLP^\ddagger (also known as MLP-PLR) use various periodic embeddings.

We provide results for more baselines in Appendix B.

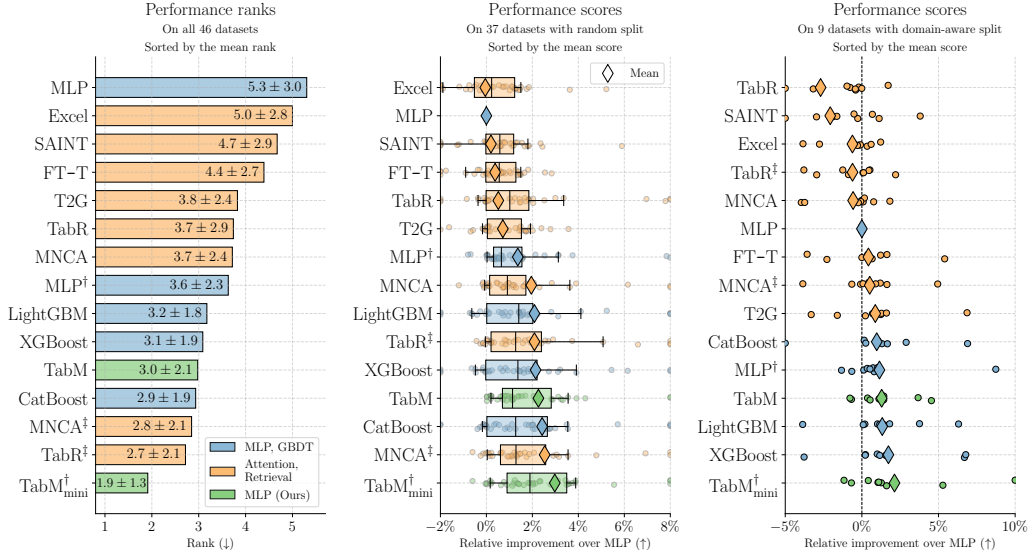


Figure 3: The task performance of tabular models on the 46 datasets from Table 1. (Left) The mean and standard deviations of the performance ranks over all datasets summarize the head-to-head comparison between the models on all datasets. (Middle & Right) The relative performance w.r.t. the plain multilayer perceptron (MLP) allows reasoning about the scale and consistency of improvements over this simple baseline. One dot of a jitter plot corresponds to the performance of a model on one of the 46 datasets. The box plots visualize the 10th, 25th, 50th, 75th and 90th percentiles of the jitter plots. Outliers are clipped. The separation in random and domain-aware dataset splits is explained in subsection 3.1.

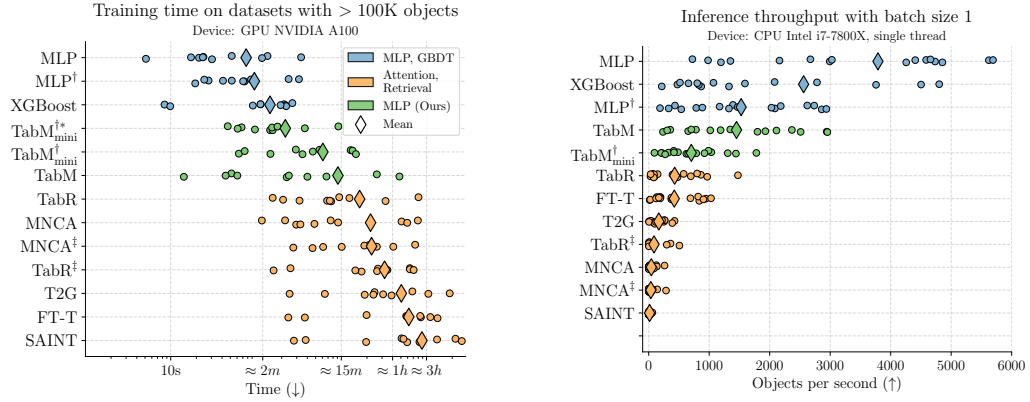


Figure 4: Training times (left) and inference throughput (right) of the models from Figure 3. One dot represents a measurement on one dataset. TabM[†]_{mini} is the optimized TabM[†]_{mini} (see subsection 4.3).

Table 2: RMSE (upper rows) and training times (lower rows) on two large datasets. The best values are in bold. The meaning of model colors follows Figure 3.

	#Objects	#Features	XGBoost	MLP	TabM [†] _{mini}	TabM [†] _{mini}	FT-T	TabR
Maps Routing	6.5M	986	0.1601 28m	0.1592 15m	0.1583 2h	0.1582 13.5h	0.1594 45.5h	OOM
Weather	13M	103	1.4234 10m	1.4842 15m	1.4090 1.3h	1.4112 3.3h	1.4409 13.5h	OOM

4.2 TASK PERFORMANCE

We evaluate all models following the protocol announced in [subsection 3.1](#), and report the results in [Figure 3](#) (see also the critical difference diagram in [Figure 9](#)). We make the following observations:

1. The performance ranks render TabM as the top-tier DL model.
2. The middle and right parts of [Figure 3](#) provide a fresh perspective on the per-dataset metrics. TabM holds its leadership among the DL models. Meanwhile, many DL methods turn out to be no better or even worse than MLP on a non-negligible number of datasets, which shows them as less reliable solutions, and changes the ranking, especially on the domain-aware splits (right).
3. One important characteristic of a model is the *weakest* part of its performance profile (e.g. the 10th or 25th percentiles in the middle plot), since it shows how reliable the model is on “inconvenient” datasets. From that perspective, MLP^\dagger seems to be a decent practical option between the plain MLP and TabM, especially given its simplicity and efficiency compared to retrieval-based alternatives, such as TabR and ModernNCA.

Summary. TabM confidently demonstrates the best performance among tabular DL models, and can serve as a reliable go-to DL baseline. This is not the case for attention- and retrieval- based models. Overall, MLP-like models, including TabM, form a representative set of tabular DL baselines.

4.3 EFFICIENCY

Now, we evaluate tabular models in terms of training and inference efficiency, which becomes a serious reality check for some of the methods. We benchmark exactly those hyperparameter configurations of models that are presented in [Figure 3](#) (see [subsection B.3](#) for the motivation).

TabM_{mini}^{†*}. Additionally, we include TabM_{mini}^{†*}, which is TabM_{mini}[†] enhanced with two efficiency-related plugins available out-of-the-box in PyTorch ([Paszke et al., 2019](#)): the automatic mixed precision (AMP) and `torch.compile` ([Ansel et al., 2024](#)). The purpose of TabM_{mini}^{†*} is to showcase the potential of the modern hardware and software for a powerful tabular DL model, and it should not be directly compared to other DL models. However, the implementation simplicity of TabM plays an important role, because it facilitates the seamless integration of the aforementioned PyTorch plugins.

Training time. We focus on training times on larger datasets, because on small datasets, all methods become almost equally affordable, regardless of the formal relative difference. Nevertheless, in [Figure 10](#), we provide measurements on small datasets as well. The left side of [Figure 4](#) reveals that TabM offers practical training times. By contrast, the long training times of attention- and retrieval-based models become one more limitation of these methods.

Inference throughput. The right side of [Figure 4](#) tells essentially the same story as the left side. In [subsection B.3](#), we also report the inference throughput on GPU with large batch sizes.

Applicability to large datasets. In [Table 2](#), we report metrics on two large datasets. As expected, attention- and retrieval-based models struggle, yielding extremely long training times, or being simply inapplicable without additional effort. See [subsection D.4](#) for implementation details.

Parameter count. Most tabular networks are overall compact. This, in particular, applies to TabM, because its size is by design comparable to MLP. We report model sizes in [subsection B.3](#).

Summary. Simple MLPs are the fastest DL models, with TabM being the runner-up. The attention- and retrieval-based models are significantly slower. Overall, MLP-like models, including TabM, form a representative set of practical and accessible tabular DL baselines.

5 ANALYSIS

5.1 PERFORMANCE AND TRAINING DYNAMICS OF THE INDIVIDUAL SUBMODELS

Recall that the prediction of TabM is defined as the mean prediction of its k implicit submodels. These submodels share almost all of their weights, and are trained simultaneously. In this section, we take a closer look at the individual performance and training dynamics of these submodels.

For the next experiment, we intentionally simplify the setup as described in detail in [subsection D.5](#). Most importantly, all models have the same depth 3 and width 512, and are trained without early stopping, i.e. the training goes beyond the optimal epochs. We use $\text{TabM}_{\text{mini}}^{k=32}$ from [Figure 1](#) with $k = 32$ denoted as $\text{TabM}_{\text{mini}}^{k=32}$. We use $\text{TabM}_{\text{mini}}^{k=1}$ (i.e. essentially one plain MLP) as a natural baseline for the submodels of $\text{TabM}_{\text{mini}}^{k=32}$, because each of the 32 submodels has the architecture of $\text{TabM}_{\text{mini}}^{k=1}$.

We visualize the training profiles on four diverse datasets (two classification and two regression problems of different sizes) in [Figure 5](#). As a reminder, the mean of the k **individual** losses is what is explicitly optimized during the training of $\text{TabM}_{\text{mini}}$, the loss of the **collective** mean prediction corresponds to how $\text{TabM}_{\text{mini}}$ makes predictions on inference, and $\text{TabM}_{\text{mini}}^{k=1}$ is just a **baseline**.

In the upper row of [Figure 5](#), the collective mean prediction of the submodels is superior to their individual predictions in terms of both training and test losses. After the initial epochs, the training loss of the baseline MLP is lower than that of the collective and individual predictions.

In the middle row of [Figure 5](#), we see a stark contrast between the individual and collective performance of the submodels. Compared to the baseline MLP, the submodels look overfitted individually, while their collective prediction exhibits substantially better generalization. This result is strict evidence of a non-trivial diversity of the submodels: without that, their collective test performance would be similar to their individual test performance. Additionally, we report the performance of the **Best** submodel of TabM over many datasets under the name $\text{TabM}[\text{B}]$ in [Figure 6](#). As such, individually, even the best submodel of TabM is no better than a simple MLP.

The lower row of [Figure 5](#) analyzes the gradient structure of $\text{TabM}_{\text{mini}}^{k=32}$. As a reminder, due to the simultaneous training and the weight sharing between the $k = 32$ submodels, most weights of $\text{TabM}_{\text{mini}}$ receive the mean of the k gradients per object on each training step. The green line in the lower row of [Figure 5](#) shows a near zero cosine similarity between these k gradients. This may explain the higher training loss of $\text{TabM}_{\text{mini}}^{k=32}$ compared to $\text{TabM}_{\text{mini}}^{k=1}$ in the first row if [Figure 5](#): perhaps, the weight sharing combined with the diverse gradients prevents $\text{TabM}_{\text{mini}}$ from (over)optimizing for the training task.

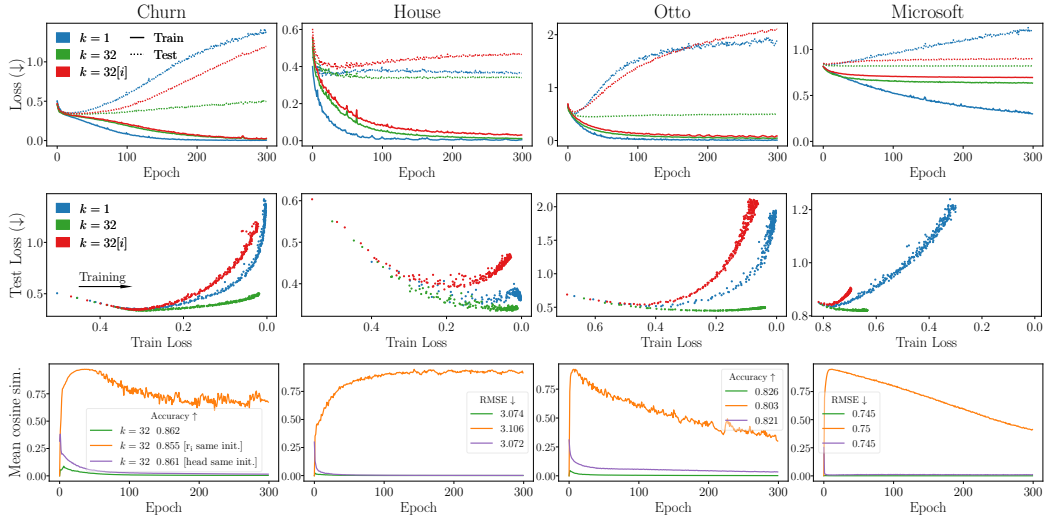


Figure 5: The training profiles of $\text{TabM}_{\text{mini}}^{k=32}$ and $\text{TabM}_{\text{mini}}^{k=1}$ as described in [subsection 5.1](#). (Upper) The training curves. $k = 32[i]$ represents the mean individual loss over the 32 submodels. (Middle) Same as the first row, but in the train-test coordinates: each dot represents some epoch from the first row, the training generally goes from left to right. This allows reasoning about overfitting by comparing test loss values for a given train loss value. (Lower) The mean pairwise cosine similarity between the k individual gradients of $\text{TabM}_{\text{mini}}^{k=32}$ with the default initialization (green) and two suboptimal initializations described in [subsection 5.1](#). Formally: $\frac{2}{n \cdot k(k-1)} \sum_{l,i,j(i < j)} \cos(g_i^l, g_j^l)$, where g_i^l is the gradient of the i -th submodel induced by the l -th of the $n = 1000$ training objects. See [subsection D.5](#) for details. The legends contain the test scores if early stopping was used.

In the same lower row of Figure 5, we run an ablation study on the two sources of submodel diversity in $\text{TabM}_{\text{mini}}$: the random initializations in the adapter R and in the k prediction heads. When all rows of R (i.e. r_i in terms of Figure 1) receive the same initialization, while the k prediction heads are initialized completely randomly (the orange line), the submodel gradients are correlated, and the task performance is poor. By contrast, the issue is less pronounced when the k prediction heads receive the same initialization, and the initialization of R is completely random (the purple line), though it also can hurt the performance. Thus, the first adapter seems to be a more impactful source of gradient diversity. Overall, we see the gradient diversity as an experimental metric requiring more exploration.

Summary. TabM draws its power from the collective prediction of weak, but diverse submodels.

5.2 SELECTING SUBMODELS AFTER TRAINING

The design of TabM allows selecting only a subset of submodels after training based on any criteria, simply by pruning extra prediction heads and the corresponding rows of the adapter matrices. To showcase this mechanics, after the training, we Greedily construct a subset of TabM’s submodels with the best collective performance on the validation set, and denote this “pruned” TabM as $\text{TabM}[\text{G}]$. The performance reported in Figure 6 shows that $\text{TabM}[\text{G}]$ is slightly behind the vanilla TabM. On average over 46 datasets, the greedy submodel selection results in 8.8 ± 6.6 submodels out of the initial $k = 32$, which can result in faster inference. See subsection D.6 for implementation details.

5.3 HOW THE PERFORMANCE OF TABM DEPENDS ON k ?

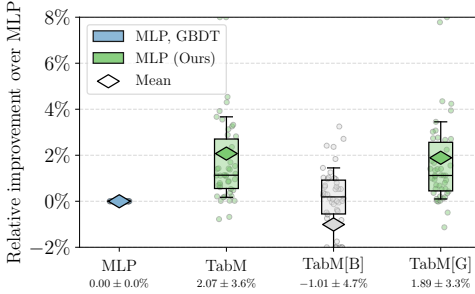


Figure 6: The performance on the 46 datasets from Table 1. $\text{TabM}[\text{B}]$ and $\text{TabM}[\text{G}]$ are described in subsection 5.1 and subsection 5.2.

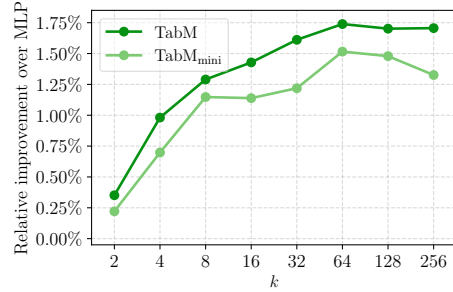


Figure 7: The average performance of TabM and $\text{TabM}_{\text{mini}}$ over 9 datasets with different values of k .

To answer the question in the title, we take TabM with the number of layers 3 and the width 512, tune the learning rate for each k separately, and report the performance in Figure 7. Based on the figure, and the results in section 4, we suggest that $k = 32$ used throughout the paper is a reasonable default value with a good balance between performance and efficiency. Also, from Figure 7, it seems that TabM accommodates large numbers of submodels more easily than $\text{TabM}_{\text{mini}}$. Perhaps, the larger number of submodel adapters in TabM provides the important additional weight capacity to fit more submodels in one model of a given size. The implementation details are available in subsection D.7.

6 CONCLUSION & FUTURE WORK

In this work, we have demonstrated that tabular multilayer perceptrons (MLPs) greatly benefit from parameter-efficient ensembling. Using this insight, we have developed TabM — a simple MLP-based model with state-of-the-art performance. In a large-scale comparison with many tabular DL models, we have demonstrated that TabM is ready to serve as a new powerful and efficient tabular DL baseline. Finally, we have analyzed the properties of the implicit submodels underlying TabM.

One idea for future work is to bring the power of (parameter-)efficient ensembles to other, non-tabular, domains with optimization-related challenges and, ideally, lightweight base models. Another idea is to evaluate TabM for uncertainty estimation and out-of-distribution (OOD) detection on tabular data, which is inspired by works like Lakshminarayanan et al. (2017).

Reproducibility statement. The code is provided in the following repository: [link](#). It contains the implementation of TabM, hyperparameter tuning scripts, evaluation scripts, configuration files with hyperparameters (the TOML files in the `exp/` directory) and the report files with the main metrics (the JSON files in the `exp/` directory). In the paper, the model is described in [section 3](#), and the implementation details are provided in [Appendix D](#).

REFERENCES

- Takuya Akiba, Shotaro Sano, Toshihiko Yanase, Takeru Ohta, and Masanori Koyama. Optuna: A next-generation hyperparameter optimization framework. In *KDD*, 2019. [19](#)
- Zeyuan Allen-Zhu and Yuanzhi Li. Towards understanding ensemble, knowledge distillation and self-distillation in deep learning. In *ICLR*, 2023. [3](#)
- Jason Ansel, Edward Yang, Horace He, Natalia Gimelshein, Animesh Jain, Michael Voznesensky, Bin Bao, Peter Bell, David Berard, Evgeni Burovski, Geeta Chauhan, Anjali Chourdia, Will Constable, Alban Desmaison, Zachary DeVito, Elias Ellison, Will Feng, Jiong Gong, Michael Gschwind, Brian Hirsh, Sherlock Huang, Kshiteej Kalambarkar, Laurent Kirsch, Michael Lazos, Mario Lezcano, Yanbo Liang, Jason Liang, Yinghai Lu, C. K. Luk, Bert Maher, Yunjie Pan, Christian Puhersch, Matthias Reso, Mark Saroufim, Marcos Yukio Siraichi, Helen Suk, Shunting Zhang, Michael Suo, Phil Tillet, Xu Zhao, Eikan Wang, Keren Zhou, Richard Zou, Xiaodong Wang, Ajit Mathews, William Wen, Gregory Chanan, Peng Wu, and Soumith Chintala. Pytorch 2: Faster machine learning through dynamic python bytecode transformation and graph compilation. In *ASPLOS*, 2024. [8](#)
- Javier Antorán, James Urquhart Allingham, and José Miguel Hernández-Lobato. Depth uncertainty in neural networks. In *NeurIPS*, 2020. [3](#)
- Sercan O. Arik and Tomas Pfister. TabNet: Attentive interpretable tabular learning. *arXiv*, 1908.07442v5, 2020. [2](#)
- Sarkhan Badirli, Xuanqing Liu, Zhengming Xing, Avradeep Bhowmik, Khoa Doan, and Sathiya S. Keerthi. Gradient boosting neural networks: GrowNet. *arXiv*, 2002.07971v2, 2020. [2](#)
- Dara Bahri, Heinrich Jiang, Yi Tay, and Donald Metzler. SCARF: Self-supervised contrastive learning using random feature corruption. In *ICLR*, 2021. [2](#)
- Jintai Chen, Jiahuan Yan, Danny Ziyi Chen, and Jian Wu. ExcelFormer: A neural network surpassing gbdt on tabular data. *arXiv*, 2301.02819v1, 2023a. [1](#), [6](#), [21](#), [25](#), [26](#)
- Kuan-Yu Chen, Ping-Han Chiang, Hsin-Rung Chou, Ting-Wei Chen, and Tien-Hao Chang. Trompt: Towards a better deep neural network for tabular data. In *ICML*, 2023b. [1](#), [2](#), [16](#)
- Tianqi Chen and Carlos Guestrin. XGBoost: A scalable tree boosting system. In *SIGKDD*, 2016. [1](#), [2](#), [6](#)
- Stanislav Fort, Huiyi Hu, and Balaji Lakshminarayanan. Deep ensembles: A loss landscape perspective. *arXiv*, 1912.02757v2, 2020. [2](#)
- Timur Garipov, Pavel Izmailov, Dmitrii Podoprikin, Dmitry P. Vetrov, and Andrew Gordon Wilson. Loss surfaces, mode connectivity, and fast ensembling of dnns. In *NeurIPS*, 2018. [3](#)
- Yury Gorishniy, Ivan Rubachev, Valentin Khrulkov, and Artem Babenko. Revisiting deep learning models for tabular data. In *NeurIPS*, 2021. [2](#), [4](#), [6](#), [16](#), [24](#), [26](#)
- Yury Gorishniy, Ivan Rubachev, and Artem Babenko. On embeddings for numerical features in tabular deep learning. In *NeurIPS*, 2022. [2](#), [5](#), [6](#), [14](#), [16](#), [21](#), [22](#), [23](#)
- Yury Gorishniy, Ivan Rubachev, Nikolay Kartashev, Daniil Shlenskii, Akim Kotelnikov, and Artem Babenko. TabR: Tabular deep learning meets nearest neighbors. In *ICLR*, 2024. [1](#), [2](#), [3](#), [6](#), [18](#), [19](#), [21](#), [23](#), [25](#), [26](#)

-
- Leo Grinsztajn, Edouard Oyallon, and Gael Varoquaux. Why do tree-based models still outperform deep learning on typical tabular data? In *NeurIPS, the "Datasets and Benchmarks" track*, 2022. 3, 18, 25
- Marton Havasi, Rodolphe Jenatton, Stanislav Fort, Jeremiah Zhe Liu, Jasper Snoek, Balaji Lakshminarayanan, Andrew Mingbo Dai, and Dustin Tran. Training independent subnetworks for robust prediction. In *ICLR*, 2021. 3, 14
- Noah Hollmann, Samuel Müller, Katharina Eggenberger, and Frank Hutter. TabPFN: A transformer that solves small tabular classification problems in a second. In *ICLR*, 2023. 1, 2, 16
- David Holzmüller, Léo Grinsztajn, and Ingo Steinwart. Better by default: Strong pre-tuned mlps and boosted trees on tabular data. *arXiv*, 2407.04491v1, 2024. 2
- Alan Jeffares, Tennison Liu, Jonathan Crabbé, Fergus Imrie, and Mihaela van der Schaar. TANGOS: Regularizing tabular neural networks through gradient orthogonalization and specialization. In *ICLR*, 2023a. 2
- Alan Jeffares, Tennison Liu, Jonathan Crabbé, and Mihaela van der Schaar. Joint training of deep ensembles fails due to learner collusion. In *NeurIPS*, 2023b. 2
- Arlind Kadra, Marius Lindauer, Frank Hutter, and Josif Grabocka. Well-tuned simple nets excel on tabular datasets. In *NeurIPS*, 2021. 2
- Guolin Ke, Qi Meng, Thomas Finley, Taifeng Wang, Wei Chen, Weidong Ma, Qiwei Ye, and Tie-Yan Liu. LightGBM: A highly efficient gradient boosting decision tree. *Advances in neural information processing systems*, 30:3146–3154, 2017. 1, 2, 6
- Myung Jun Kim, Léo Grinsztajn, and Gaël Varoquaux. CARTE: pretraining and transfer for tabular learning. *arXiv*, abs/2402.16785v1, 2024. 17
- Günter Klambauer, Thomas Unterthiner, Andreas Mayr, and Sepp Hochreiter. Self-normalizing neural networks. In *NIPS*, 2017. 2, 16
- Jannik Kossen, Neil Band, Clare Lyle, Aidan N. Gomez, Tom Rainforth, and Yarin Gal. Self-attention between datapoints: Going beyond individual input-output pairs in deep learning. In *NeurIPS*, 2021. 2
- Balaji Lakshminarayanan, Alexander Pritzel, and Charles Blundell. Simple and scalable predictive uncertainty estimation using deep ensembles. In *NeurIPS*, 2017. 3, 10, 14
- Olivier Laurent, Adrien Lafage, Enzo Tartaglione, Geoffrey Daniel, Jean-Marc Martinez, Andrei Bursuc, and Gianni Franchi. Packed ensembles for efficient uncertainty estimation. In *ICLR*, 2023. 4
- Stefan Lee, Senthil Purushwalkam, Michael Cogswell, David J. Crandall, and Dhruv Batra. Why M heads are better than one: Training a diverse ensemble of deep networks. *arXiv*, abs/1511.06314, 2015. 3, 14
- Ilya Loshchilov and Frank Hutter. Decoupled weight decay regularization. In *ICLR*, 2019. 19
- Sascha Marton, Stefan Lüdtke, Christian Bartelt, and Heiner Stuckenschmidt. GRANDE: Gradient-based decision tree ensembles for tabular data. In *ICLR*, 2024. 2
- Adam Paszke, Sam Gross, Francisco Massa, Adam Lerer, James Bradbury, Gregory Chanan, Trevor Killeen, Zeming Lin, Natalia Gimelshein, Luca Antiga, Alban Desmaison, Andreas Köpf, Edward Z. Yang, Zachary DeVito, Martin Raison, Alykhan Tejani, Sasank Chilamkurthy, Benoit Steiner, Lu Fang, Junjie Bai, and Soumith Chintala. PyTorch: An imperative style, high-performance deep learning library. In *NeurIPS*, 2019. 8
- F. Pedregosa, G. Varoquaux, A. Gramfort, V. Michel, B. Thirion, O. Grisel, M. Blondel, P. Prettenhofer, R. Weiss, V. Dubourg, J. Vanderplas, A. Passos, D. Cournapeau, M. Brucher, M. Perrot, and E. Duchesnay. Scikit-learn: Machine learning in Python. *Journal of Machine Learning Research*, 12:2825–2830, 2011. 19

-
- Sergei Popov, Stanislav Morozov, and Artem Babenko. Neural oblivious decision ensembles for deep learning on tabular data. In *ICLR*, 2020. 2
- Liudmila Prokhorenkova, Gleb Gusev, Aleksandr Vorobev, Anna Veronika Dorogush, and Andrey Gulin. CatBoost: unbiased boosting with categorical features. In *NeurIPS*, 2018. 1, 2, 6
- Tao Qin and Tie-Yan Liu. Introducing LETOR 4.0 datasets. *arXiv*, 1306.2597v1, 2013. 3
- Ivan Rubachev, Artem Alekberov, Yury Gorishniy, and Artem Babenko. Revisiting pretraining objectives for tabular deep learning. *arXiv*, 2207.03208v1, 2022. 2
- Ivan Rubachev, Nikolay Kartashev, Yury Gorishniy, and Artem Babenko. TabReD: Analyzing Pitfalls and Filling the Gaps in Tabular Deep Learning Benchmarks. *arXiv*, 2406.19380v4, 2024. 1, 3, 18, 19, 20, 23, 25, 26
- Gowthami Somepalli, Micah Goldblum, Avi Schwarzschild, C. Bayan Bruss, and Tom Goldstein. SAINT: improved neural networks for tabular data via row attention and contrastive pre-training. *arXiv*, 2106.01342v1, 2021. 2, 6, 25
- Weiping Song, Chence Shi, Zhiping Xiao, Zhijian Duan, Yewen Xu, Ming Zhang, and Jian Tang. AutoInt: Automatic feature interaction learning via self-attentive neural networks. In *CIKM*, 2019. 2, 16, 26
- Nitish Srivastava, Geoffrey E. Hinton, Alex Krizhevsky, Ilya Sutskever, and Ruslan Salakhutdinov. Dropout: a simple way to prevent neural networks from overfitting. *Journal of Machine Learning Research*, 15(1):1929–1958, 2014. 5
- Ilya O. Tolstikhin, Neil Houlsby, Alexander Kolesnikov, Lucas Beyer, Xiaohua Zhai, Thomas Unterthiner, Jessica Yung, Andreas Steiner, Daniel Keysers, Jakob Uszkoreit, Mario Lucic, and Alexey Dosovitskiy. Mlp-mixer: An all-mlp architecture for vision. In *NeurIPS*, 2021. 6, 16
- Mehmet Ozgur Turkoglu, Alexander Becker, Hüseyin Anil Gündüz, Mina Rezaei, Bernd Bischl, Rodrigo Caye Daudt, Stefano D’Aronco, Jan D. Wegner, and Konrad Schindler. Film-ensemble: Probabilistic deep learning via feature-wise linear modulation. In *NeurIPS 2022*, 2022. 3, 14, 15
- Ashish Vaswani, Noam Shazeer, Niki Parmar, Jakob Uszkoreit, Llion Jones, Aidan N. Gomez, Lukasz Kaiser, and Illia Polosukhin. Attention is all you need. In *NIPS*, 2017. 6
- Ruoxi Wang, Rakesh Shivanna, Derek Z. Cheng, Sagar Jain, Dong Lin, Lichan Hong, and Ed H. Chi. Dcn v2: Improved deep & cross network and practical lessons for web-scale learning to rank systems. *arXiv*, 2008.13535v2, 2020. 2, 16
- Yeming Wen, Dustin Tran, and Jimmy Ba. Batchensemble: an alternative approach to efficient ensemble and lifelong learning. In *ICLR*, 2020. 2, 3, 4, 5, 14, 15
- Jiahuan Yan, Jintai Chen, Yixuan Wu, Danny Z. Chen, and Jian Wu. T2G-FORMER: organizing tabular features into relation graphs promotes heterogeneous feature interaction. In *AAAI*, 2023. 2, 6, 25
- Han-Jia Ye, Huai-Hong Yin, and De-Chuan Zhan. Modern neighborhood components analysis: A deep tabular baseline two decades later. *arXiv*, 2407.03257v1, 2024. 2, 6, 21, 23
- Shaofeng Zhang, Meng Liu, and Junchi Yan. The diversified ensemble neural network. In *NeurIPS*, 2020. 3

A ADDITIONAL DISCUSSION ON TABM

A.1 MOTIVATION

Why BatchEnsemble? Among relatively ease-to-use “efficient ensembling” methods, beyond BatchEnsemble, there are examples such as dropout ensembles (Lakshminarayanan et al., 2017), naive multi-head architectures, TreeNet (Lee et al., 2015). However, in the literature, they were consistently outperformed by more advanced methods, including BatchEnsemble (Wen et al., 2020), MIMO (Havasi et al., 2021), FiLM-Ensemble (Turkoglu et al., 2022).

Among advanced methods, BatchEnsemble seems to be one of the simplest and most flexible options. For example, FiLM-Ensemble (Turkoglu et al., 2022) requires normalization layers to be presented in the original architecture, which is not always the case for tabular MLPs. MIMO (Havasi et al., 2021), in turn, imposes additional limitations compared to BatchEnsemble. *First*, it requires *concatenating* (not *stacking*, as with BatchEnsemble) all k input representations, which increases the input size of the first linear layer. With the relatively high number of submodels $k = 32$ used in our paper, this can be an issue on datasets with a large number of features, and especially when feature embeddings (Gorishniy et al., 2022) are used. For example, for $k = 32$, the number of features $m = 1000$ and the feature embedding size $l = 32$, the input size approaches one million resulting in an extremely large first linear layer of MLP. *Second*, with BatchEnsemble, it is easy to explicitly materialize, analyze and prune individual submodels. By contrast, in MIMO, all submodels are implicitly entangled within one MLP, and there is no easy way to access individual submodels.

Why MLPs? Despite the applicability of BatchEnsemble (Wen et al., 2020) to almost any architecture, we focus specifically on MLPs. The key reason is *efficiency*. *First*, to achieve high performance, throughout the paper, we use the relatively large number of submodels $k = 32$. However, the desired less-than- $\times k$ runtime overhead of BatchEnsemble typically happens only when the original model underutilizes the power of parallel computations of a given hardware. This will not be the case for attention-based models on datasets with a large number of features, as well as for retrieval-based models on datasets with a large number of objects. *Second*, as we show in subsection 4.3, attention- and retrieval-based models are already slow as-is. By contrast, MLPs are exceptionally efficient, to the extent that slowing them down even by an order of magnitude will still result in practical models.

Also, generally speaking, the definition of MLP suggested in subsection 3.3 and used in TabM is not special, and more advanced MLP-like backbones can be used. However, in preliminary experiments, we did not observe the benefits of more advanced backbones. Perhaps, small technical differences between backbones become less impactful in the context of parameter-efficient ensembling, at least in the scope of middle-to-large-sized datasets.

A.2 WHY TABM OUTPERFORMS A FULL-FLEDGED DEEP ENSEMBLE?

As shown in Figure 2, TabM_{naive}, TabM and TabM_{mini} are all superior to $\text{MLP}^{\times k}$ — the full-fledged ensemble of k MLPs. Moreover, the performance gap is significant. To the best of our knowledge, this result is rather not expected, because the literature on efficient ensembles is usually focused on catching up with deep ensembles, not on outperforming them, let alone significantly outperforming them. Plus, after the training, TabM can be explicitly materialized as a traditional ensemble of k MLPs. With that in mind, we highlight three hypotheses for the superior performance of TabM compared to $\text{MLP}^{\times k}$. The first one relies on the analysis from subsection 5.1, and the other two are more general.

First, we highlight the combination of the weight sharing and gradient diversity (observed in the third row of Figure 5) in TabM. Perhaps, the regularization power of the weakly aligned individual gradients cannot be recovered by technical details such as hyperparameter tuning, training protocol, etc. In this case, we can say that MLP ensembles seem to win from this regularization when training on tabular data. This, in turn, can be related to the common belief that optimization on tabular data is challenging, especially for MLPs. Overall, it is unclear if the phenomenon will generalize to other models and/or domains.

Second, the hyperparameter tuning for $\text{MLP}^{\times k}$ may be suboptimal. Recall that, in Figure 2, we tune hyperparameters of one ensemble-unaware MLP, and then train the tuned MLP from scratch k times

to obtain $\text{MLP}^{\times k}$. Perhaps, if the hyperparameters are tuned directly for $\text{MLP}^{\times k}$, then more powerful (and exotic) configurations can be found. However, that would make the tuning $\times k$ more expensive.

Third, the parallel training (and, in particular, early stopping) of the implicit submodels in TabM may be important. The direct analogy for $\text{MLP}^{\times k}$ would be to train all k members in parallel on the same training batches. In [Figure 2](#), all members $\text{MLP}^{\times k}$ are trained independently under different random seeds (and, in particular, over different training batch sequences).

A.3 TABM WITH FEATURE EMBEDDINGS

Here, we provide additional implementation details for $\text{TabM}_{\text{mini}}^{\dagger}$ and TabM^{\dagger} introduced in [subsection 3.3](#). In fact, there are no changes in the usage of feature embeddings compared to plain MLPs.

Technically, feature embeddings are applied, and the result is flattened, before the `Clone` module in terms of [Figure 1](#). For example, if a dataset has m continuous features and all of them are embedded, the very first adapter R will have the shape $k \times m d_e$, where d_e is the feature embedding size. For $\text{TabM}_{\text{mini}}^{\dagger}$ and TabM^{\dagger} , we initialize the first multiplicative adapter R of the first linear layer from the standard normal distribution $\mathcal{N}(0, 1)$. The remaining details are best understood from the source code.

A.4 HYPERPARAMETERS

As mentioned in the main text, we noticed that the typical optimal learning rate for TabM is higher than for MLP (we share the tuned hyperparameters on all datasets in the repository, so the precise comparison is possible). We hypothesize that the reason is the effectively larger batch size because of the `Clone` operation (see [Figure 1](#)), which, in particular, leads to the k mostly orthogonal gradients per object (see [subsection 5.1](#)) on each training step. The latter leads to lower gradient norms after averaging the k gradients, which can be related to the need for larger learning rates.

A.5 LIMITATIONS AND PRACTICAL CONSIDERATIONS

TabM does not introduce any new limitations compared to BatchEnsemble ([Wen et al., 2020](#)). Nevertheless, we note the following:

- The MLP backbone used in TabM is one of the simplest possible, and generally, more advanced backbones can be used. That said, some backbones may require additional care when used in TabM. For example, we did not explore backbones with normalization layers. For such layers, it is possible to allocate non-shared trainable affine transformations for each implicit submodel by adding one multiplicative and one additive adapter after the normalization layer (i.e. like in FiLM-Ensemble ([Turkoglu et al., 2022](#))). Additional experiments are required to find the best strategy.
- Arguably the key limitation is that BatchEnsemble-like techniques are not “local”, but instead affect the whole model starting from the first modified layer. Namely, when the computation flow hits the first modified layer, the k prediction branches are created, and the rest of the network will have to make k times more computations. This can be easily affordable for small base models, but may be less affordable for heavy base models.
- For ensemble-like models, such as TabM, the notion of “the final object embedding” changes: now, it is not a single vector, but a set of k vectors. This can be important for scenarios when TabM is used for solving more than one task, in particular, when it is pretrained as a generic feature extractor and then reused for other tasks. The main practical guideline is that the k prediction branches should *never* interact with each other (e.g. through attention, pooling, etc.) and should always be trained separately.

B EXTENDED RESULTS

This section complements [section 4](#).

B.1 ADDITIONAL BASELINES

In addition to [subsection 4.1](#), we consider the following models:

- MLP-PLR [Gorishniy et al. \(2022\)](#), that is, an MLP with periodic embeddings.
- ResNet ([Gorishniy et al., 2021](#))
- SNN ([Klambauer et al., 2017](#))
- DCNv2 ([Wang et al., 2020](#))
- AutoInt ([Song et al., 2019](#))
- MLP-Mixer is our adaptation of [Tolstikhin et al. \(2021\)](#) for tabular data.
- Trompt ([Chen et al., 2023b](#)) (our reimplement, since there is no official implementation)

We also evaluated TabPFN ([Hollmann et al., 2023](#)), where possible. The results for this model are available only in [Appendix E](#), because this model is by design not applicable to regression tasks, which is a considerable number of our datasets. Overall, TabPFN specializes on small datasets. In line with that, the performance of TabPFN on our benchmark was not competitive.

B.2 TASK PERFORMANCE

[Figure 8](#) is a different version of [Figure 3](#) with additional baselines. Overall, none of the additional baselines affects our main story.

[Figure 9](#) is the critical difference diagram (CDD) computed over exactly the same results that were used for building [Figure 3](#).

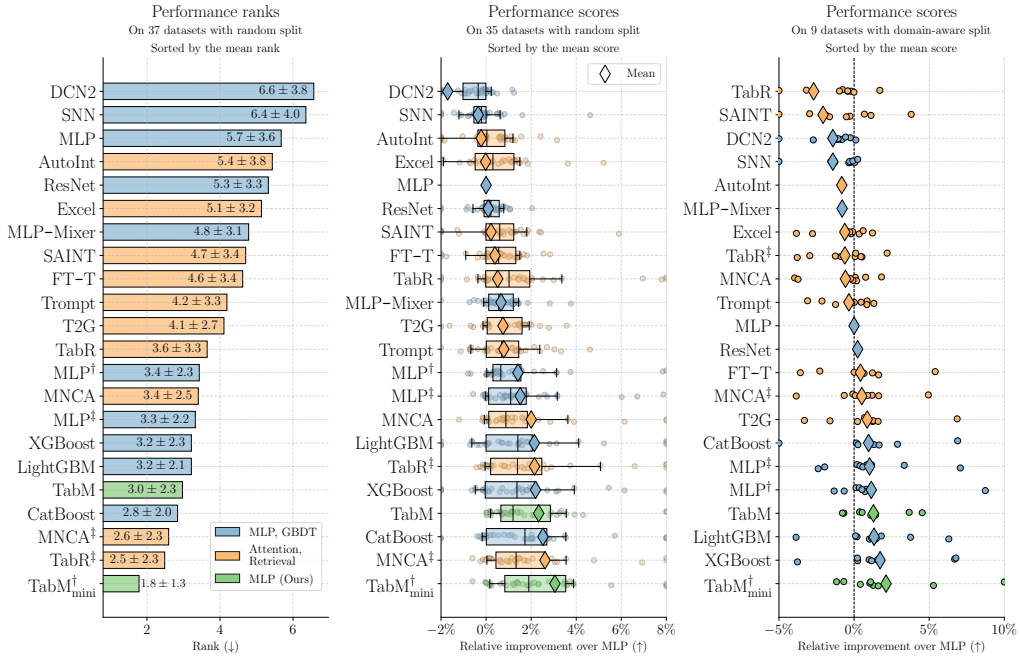


Figure 8: An extended comparison of tabular models as in [Figure 3](#). Note that the ranks (left) are computed only over the 37 datasets with random splits, because ResNet, AutoInt and MLP-Mixer were evaluated only on one 1 out of 9 datasets with domain-aware splits.

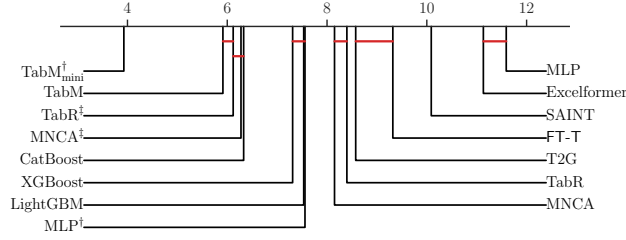


Figure 9: Critical difference diagram. The computation method is taken from the [Kim et al. \(2024\)](#).

B.3 EFFICIENCY

This section complements [subsection 4.3](#).

Additional results.

[Figure 10](#) complements [Figure 4](#) by providing the training times on smaller datasets and the inference throughput on GPU with large batch sizes.

[Table 3](#) provide the number of trainable parameters for some of the models from [Figure 3](#).

Motivation for the benchmark setup. Comparing models under all possible kinds of budgets (task performance, the number of parameters, training time, etc.) on all possible hardware (GPU, CPU, etc.) with all possible batch sizes is rather infeasible. As such, we set a narrow goal of *providing a high-level intuition on the efficiency in a transparent setting*. Thus, benchmarking the transparently obtained tuned hyperparameter configurations works well for our goal. Yet, this choice also has a limitation: the hyperparameter tuning process is not aware of the efficiency budget, so it can prefer much heavier configurations even if they lead to tiny performance improvements, which will negatively affect efficiency without a good reason. Overall, we hope that the large number of datasets compensates for potentially imperfect per-dataset measurements.

Motivation for the two setups for measuring inference throughput.

- The setup in the right side of [Figure 4](#) simulates the online per-object predictions.
- The setup in the right side of [Figure 10](#) simulates the offline batched computations.

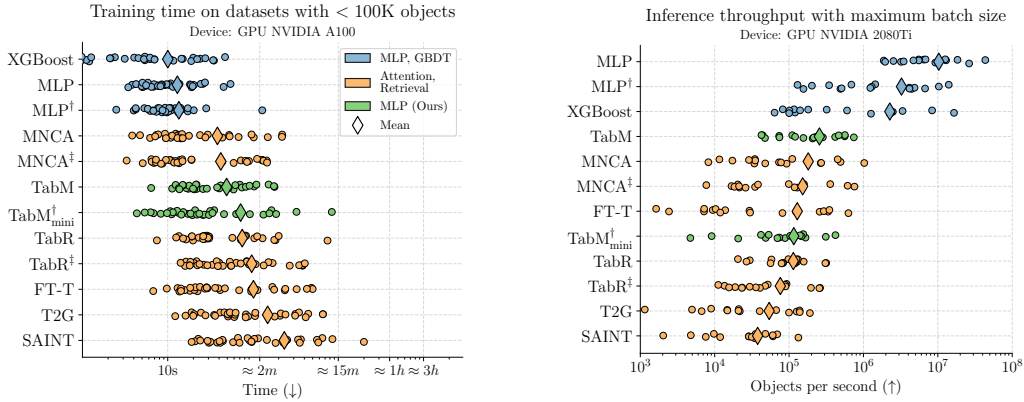


Figure 10: (Left) Training time on datasets with less than 100K objects. (Right) Inference throughput on GPU with maximum possible batch size (i.e. the batch size depends of a model).

Table 3: Mean number of parameters with std. dev. for 7 different tuned models across all 46 datasets.

TabM	MLP	FT-T	T2G	TabR	ModernNCA	SAINT
$1.4M \pm 1.3M$	$1.0M \pm 1.0M$	$1.2M \pm 1.2M$	$2.1M \pm 1.6M$	$858K \pm 1.4M$	$1.0M \pm 1.1M$	$175.4M \pm 565.4M$

C DATASETS

In total, we use 46 datasets:

1. 38 datasets are taken from [Gorishniy et al. \(2024\)](#), which includes:
 - (a) 28 datasets from [Grinsztajn et al. \(2022\)](#). See the original paper for the precise dataset information.
 - (b) 10 datasets from other sources. Their properties are provided in [Table 4](#).
2. 8 datasets are taken from [Rubachev et al. \(2024\)](#). Their properties are provided in [Table 5](#).

In fact, the aforementioned 38 datasets from [Gorishniy et al. \(2024\)](#) is only a subset of the datasets used in [Gorishniy et al. \(2024\)](#). Namely, we did not include the following of the remaining datasets:

- The datasets that, according to [Rubachev et al. \(2024\)](#), have incorrect splits and/or label leakage, including: Bike.Sharing.Demand, compass, electricity, SGEMM.GPU.kernel.performance, sulfur, visualizing_soil, and the weather forecasting dataset (it is replaced by the correct weather forecasting dataset from [Rubachev et al. \(2024\)](#)).
- rl from ([Grinsztajn et al., 2022](#)). We observed abnormal results on these datasets. This is an anonymous dataset, which made the investigation impossible, so we removed this dataset to avoid confusion.
- yprop_4.1 from ([Grinsztajn et al., 2022](#)). Strictly speaking, this dataset was omitted due to a mistake on our side. For future work, we note that the typical performance gaps on this dataset have low absolute values in terms of RMSE. Perhaps, R^2 may be a more appropriate metric for this dataset.

Table 4: Properties of those datasets from [Gorishniy et al. \(2024\)](#) that are not part of [Grinsztajn et al. \(2022\)](#) or [Rubachev et al. \(2024\)](#). “# Num”, “# Bin”, and “# Cat” denote the number of numerical, binary, and categorical features, respectively. The table is taken from ([Gorishniy et al., 2024](#)).

Name	# Train	# Validation	# Test	# Num	# Bin	# Cat	Task type	Batch size
Churn Modelling	6 400	1 600	2 000	10	3	1	Binclass	128
California Housing	13 209	3 303	4 128	8	0	0	Regression	256
House 16H	14 581	3 646	4 557	16	0	0	Regression	256
Adult	26 048	6 513	16 281	6	1	8	Binclass	256
Diamond	34 521	8 631	10 788	6	0	3	Regression	512
Otto Group Products	39 601	9 901	12 376	93	0	0	Multiclass	512
Higgs Small	62 751	15 688	19 610	28	0	0	Binclass	512
Black Friday	106 764	26 692	33 365	4	1	4	Regression	512
Covertypes	371 847	92 962	116 203	15	4	1	Multiclass	1024
Microsoft	723 412	235 259	241 521	131	5	0	Regression	1024

Table 5: Properties of the datasets from the TabReD benchmark ([Rubachev et al., 2024](#)). “# Num”, “# Bin”, and “# Cat” denote the number of numerical, binary, and categorical features, respectively.

Name	# Train	# Validation	# Test	# Num	# Bin	# Cat	Task type	Batch size
Sberbank Housing	18 847	4 827	4 647	365	17	10	Regression	256
Ecom Offers	109 341	24 261	26 455	113	6	0	Binclass	1024
Maps Routing	160 019	59 975	59 951	984	0	2	Regression	1024
Homesite Insurance	224 320	20 138	16 295	253	23	23	Binclass	1024
Cooking Time	227 087	51 251	41 648	186	3	3	Regression	1024
Homecredit Default	267 645	58 018	56 001	612	2	82	Binclass	1024
Delivery ETA	279 415	34 174	36 927	221	1	1	Regression	1024
Weather	106 764	42 359	40 840	100	3	0	Regression	1024

D IMPLEMENTATION DETAILS

D.1 HARDWARE

Most of the experiments were conducted on a single NVIDIA A100 GPU. In rare exceptions, we used a machine with a single NVIDIA 2080 Ti GPU and Intel(R) Core(TM) i7-7800X CPU @ 3.50GHz.

D.2 EXPERIMENT SETUP

We mostly follow the experiment setup from [Gorishniy et al. \(2024\)](#). As such, some of the text below is copied from ([Gorishniy et al., 2024](#)).

Data preprocessing. For each dataset, for all DL-based solutions, the same preprocessing was used for fair comparison. For numerical features, by default, we used a slightly modified version of the quantile normalization from the Scikit-learn package ([Pedregosa et al., 2011](#)) (see the source code), with rare exceptions when it turned out to be detrimental (for such datasets, we used the standard normalization or no normalization). For categorical features, we used one-hot encoding. Binary features (i.e. the ones that take only two distinct values) are mapped to $\{0, 1\}$ without any further preprocessing. We completely follow [Rubachev et al. \(2024\)](#) on [Table 5](#) datasets.

Training neural networks. For DL-based algorithms, we minimize cross-entropy for classification problems and mean squared error for regression problems. We use the AdamW optimizer ([Loshchilov & Hutter, 2019](#)). We do not apply learning rate schedules. We do not use data augmentations. We apply global gradient clipping to 1.0. For each dataset, we used a predefined dataset-specific batch size. We continue training until there are `patience` consecutive epochs without improvements on the validation set; we set `patience` = 16 for the DL models.

Hyperparameter tuning. In most cases, hyperparameter tuning is performed with the TPE sampler (typically, 50-100 iterations) from the Optuna package ([Akiba et al., 2019](#)). Hyperparameter tuning spaces for most models are provided in individual sections below (example for TabM: [subsection D.9](#)). We follow [Rubachev et al. \(2024\)](#) and use 25 iterations on some datasets from [Table 5](#).

Evaluation. On a given dataset, for a given model, the tuned hyperparameters are evaluated under multiple (in most cases, 15) random seeds. The mean test metric and its standard deviation over these random seeds are then used to compare algorithms as described in [subsection D.3](#).

D.3 METRICS

We use Root Mean Squared Error for regression tasks, ROC-AUC for classification datasets from [Table 5](#) (following [Rubachev et al. \(2024\)](#)), and accuracy for the rest of datasets (following [Gorishniy et al. \(2024\)](#)). We also tried computing ROC-AUC for all classification datasets, but did not observe any significant changes (see [Figure 11](#)), so we stuck to prior work. By default, the mean test score and its standard deviation are obtained by training a given model with tuned hyperparameters from scratch on a given dataset under 15 different random seeds.

How we compute ranks. Our method of computing ranks does not count small improvements as wins, hence the reduced range of ranks compared to other studies. Intuitively, our ranks can be considered as “tiers”.

Assume the higher the score the better and `mean_score_Ref` > `mean_score_A`. Then reference `Model_Ref` and `Model_A` are equal (have the same rank) if $(\text{mean_score_Ref} - \text{mean_score_A}) \leq \text{std_Ref}$. To assign ranks, we sort models in descending score order. Starting from the best model (with rank equal to 1) we iterate over models and assign first rank to all models that are equal to the best model according to the mentioned definition. The first model in descending order that is not equal to the best model is assigned with second rank and becomes a new reference model. We continue the process until all models are ranked. Ranks are computed independently for each dataset.

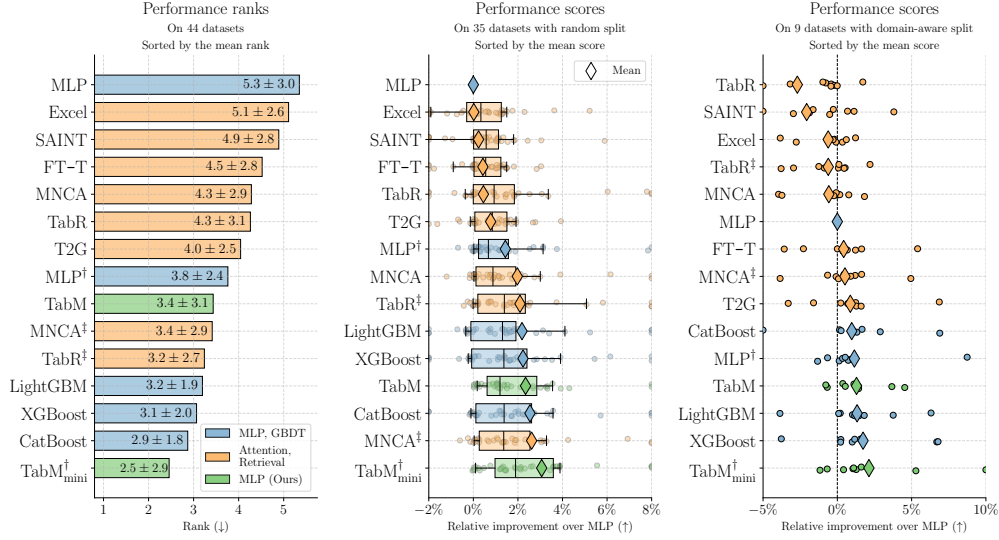


Figure 11: Same as Figure 3, but ROC-AUC is used as the metric for all classification datasets. The two multiclass datasets presented in our benchmark are not taken into account.

D.4 IMPLEMENTATION DETAILS OF SUBSECTION 4.3

Applicability to large datasets. The two datasets used in Table 2 are the full versions of the “Weather” and “Maps Routing” datasets from Rubachev et al. (2024). Their smaller versions with subsampled training set were already included in Table 1, and were used when building Figure 3. The validation and test sets are the same for the small and large versions of these datasets, so the task metrics are comparable between the two versions. When running models on the large versions of the datasets, we reused the hyperparameters tuned for their small versions. Thus, this experiment can be seen as a quick assessment of the applicability of several tabular DL to large datasets, without a strong focus on the task performance. All models, except for FT-Transformer, were evaluated under 3 random seeds. FT-Transformer was evaluated under 1 random seed.

D.5 IMPLEMENTATION DETAILS OF SUBSECTION 5.1

Experiment setup. This paragraph complements the description of the experiment setup in subsection 5.1. Namely, in addition to what is mentioned in the main text:

- Dropout and weight decay are turned off.
- To get representative training profiles for all models, the learning rates are tuned separately for $\text{TabM}_{\text{mini}}^{k=1}$ and $\text{TabM}_{\text{mini}}^{k=32}$ on validation sets using the usual metrics (i.e. RMSE or accuracy) as the guidance. The grid for learning rate tuning was: `numpy.logspace(numpy.log10(1e-5), numpy.log10(5e-3), num=25)`.
- The adapter R in $\text{TabM}_{\text{mini}}$ is initialized from $N(0, 1)$ instead of ± 1 . We observed that ± 1 resulted in occasional minor jumps in some of the curves shown in Figure 5. The number and magnitude of the jumps were low and had no effect on the story. However, in line with all other changes to the experiment setup in this section, we adjusted the initialization to avoid the jumps, to ensure that the training runs were not disturbed by side-effects of unknown nature.

Cosine similarity between the k gradients. This paragraph complements the story about the third row of Figure 5. The reported cosine similarity between the k gradients was computed as follows. Before the training, we randomly select $n = 1000$ training objects — these reference objects stay the same during the whole training run. During the training, at the start of every epoch, we calculate the metric according to the formula in the caption of Figure 5:

1. First, for each of the n reference objects, we compute the k individual gradients, and omit the gradient components related to the weights of the prediction heads. Thus, the size of one

gradient equals the number of all parameters, minus the number of parameters in one prediction head.

2. Then for each of the n reference objects, we compute the $\frac{k(k-1)}{2}$ pairwise cosine similarities between the k individual gradients.
3. Finally, we average the cosine similarities over all pairs of gradients over all reference objects, which gives the formula in the caption of Figure 5.

Limitations. Continuing the story about the gradient diversity, we note that in high-dimensional spaces, the near-zero values of cosine similarity can be hard to interpret, which is a potential limitation of our analysis. That said, a non-trivial positive (negative) value is rather a decent indicator of a non-trivial positive (negative) correlation between vectors.

D.6 IMPLEMENTATION DETAILS OF SUBSECTION 5.2

TabM[G]. Here, we clarify the implementation details for TabM[G] described in subsection 5.2. TabM[G] is obtained from a trained TabM by greedily selecting submodels from TabM starting from the best one and stopping when two conditions are simultaneously true for the first time: (1) adding any new submodel does not improve the validation metric of the collective prediction; (2) the current validation metric is already better than that of the initial model with all k submodels. To clarify, during the greedy selection, the i -th submodel is considered to be better than the j -th submodel if adding the i -th submodel to the aggregated prediction leads to better validation metrics (i.e. it is *not* the same as adding the submodel in the order of their individual validation metrics).

D.7 IMPLEMENTATION DETAILS OF SUBSECTION 5.3

Figure 7 shows the mean percentage improvements (see subsection D.3) over MLP across 9 datasets from Table 4 (without Coverttype). We have used a TabM_{mini} with 3 hidden layers of the width $d = 512$, the dropout rate 0.1 and tuned learning rate for different k . The score on each dataset is averaged over 5 seeds.

D.8 NON-LINEAR EMBEDDINGS FOR CONTINUOUS FEATURES

Notation. We use the notation based on \dagger and \ddagger only for brevity. Any other unambiguous notation can be used in future work.

Updated piecewise-linear embeddings. We use a slightly different implementation of the piecewise-linear embeddings compared to Gorishniy et al. (2022). Architecture-wise, our implementation corresponds to the “Q-L” and “T-L” variations from Table 2 in Gorishniy et al. (2022) (we use the quantile-based bins for simplicity). In practice, our implementation is significantly faster, and uses a different parametrization and initialization. See the source code for details.

TabM. For TabM, we recommend the aforementioned updated piecewise-linear embeddings as the default embedding architecture. This corresponds to the TabM_{mini}[†] and TabM[†] models.

Other models. Since it is not feasible to test all combinations of backbones and embeddings, for baselines, we stick to the embeddings used in the original papers (applies to TabR (Gorishniy et al., 2024), ExcelFormer (Chen et al., 2023a) and ModernNCA (Ye et al., 2024)). For all models with feature embeddings (including TabM, MLP, TabR, ModernNCA, ExcelFormer), the embeddings-related details are commented in the corresponding sections below.

D.9 TABM

Feature embeddings. TabM_{mini}[†] and TabM[†] are the versions of TabM with non-linear feature embeddings. TabM_{mini}[†] and TabM[†] use the updated piecewise-linear feature embeddings mentioned in subsection D.8.

Table 6 provides the hyperparameter tuning spaces for TabM and TabM_{mini}. Table 7 provides the hyperparameter tuning spaces for TabM[†] and TabM_{mini}[†].

Table 6: The hyperparameter tuning space for TabM and TabM_{mini}. Here, (B) = {Coverttype, Microsoft, Table 5} and (A) contains all other datasets.

Parameter	Distribution or Value
k	32
# layers	UniformInt[1, 5]
Width (hidden size)	UniformInt[64, 1024]
Dropout rate	{0.0, Uniform[0.0, 0.5]}
Learning rate	LogUniform[1e-4, 5e-3]
Weight decay	{0, LogUniform[1e-4, 1e-1]}
# Tuning iterations	(A) 100 (B) 50

Table 7: The hyperparameter tuning space for TabM_{mini}[†] and TabM[†]. Here, (B) = {Coverttype, Microsoft, Table 5} and (A) contains all other datasets.

Parameter	Distribution or Value
k	32
# layers	UniformInt[1, 4]
Width (hidden size)	UniformInt[64, 1024]
Dropout rate	{0.0, Uniform[0.0, 0.5]}
# PLE bins	UniformInt[8, 32]
Learning rate	LogUniform[5e-5, 3e-3]
Weight decay	{0, LogUniform[1e-4, 1e-1]}
# Tuning iterations	(A) 100 (B) 50

D.10 MLP

Feature embeddings. MLP[†] and MLP[‡] are the versions of MLP with non-linear feature embeddings. MLP[†] uses the updated piecewise-linear embeddings mentioned in subsection D.8. MLP[‡] (also known as MLP-PLR) uses the periodic embeddings (Gorishniy et al., 2022). Tehcnically, it is the PeriodicEmbeddings class from the rtdl.num_embeddings Python package. We tested two variations: with lite=False and lite=True. In the paper, only the former one is reported, but in the source code, the results for both are available.

Table 8, Table 9, Table 10 provide the hyperparameter tuning spaces for MLP, MLP[†] and MLP[‡], respectively.

Table 8: The hyperparameter tuning space for MLP.

Parameter	Distribution
# layers	UniformInt[1, 6]
Width (hidden size)	UniformInt[64, 1024]
Dropout rate	{0.0, Uniform[0.0, 0.5]}
Learning rate	LogUniform[3e-5, 1e-3]
Weight decay	{0, LogUniform[1e-4, 1e-1]}
# Tuning iterations	100

Table 9: The hyperparameter tuning space for MLP[†].

Parameter	Distribution
# layers	UniformInt[1, 5]
Width (hidden size)	UniformInt[64, 1024]
Dropout rate	{0.0, Uniform[0.0, 0.5]}
Learning rate	LogUniform[3e-5, 1e-3]
Weight decay	{0, LogUniform[1e-4, 1e-1]}
d_embedding	UniformInt[8, 32]
n_bins	UniformInt[2, 128]
# Tuning iterations	100

Table 10: The hyperparameter tuning space for MLP[‡].

Parameter	Distribution
# layers	UniformInt[1, 5]
Width (hidden size)	UniformInt[64, 1024]
Dropout rate	{0.0, Uniform[0.0, 0.5]}
Learning rate	LogUniform[3e-5, 1e-3]
Weight decay	{0, LogUniform[1e-4, 1e-1]}
n_frequencies	UniformInt[16, 96]
d_embedding	UniformInt[16, 32]
frequency_init_scale	LogUniform[1e-2, 1e1]
# Tuning iterations	100

D.11 TABR

Feature embeddings. TabR[‡] is the version of TabR with non-linear feature embeddings. TabR[‡] uses the periodic embeddings (Gorishniy et al., 2022), specifically, `PeriodicEmbeddings(lite=True)` from the `rtdl_num_embeddings` Python package on most datasets. On the datasets from Table 5, TabR[‡] uses the `PeriodicEmbeddings(lite=True)` embeddings on the Sberbank Housing and Ecom Offers datasets, and `LinearReLUEmbeddings` on the rest (to fit the computations into the GPU memory, following the original TabR paper).

Since we follow the training and evaluation protocols from Gorishniy et al. (2024), and TabR was proposed in Gorishniy et al. (2024), we simply reuse the results for TabR. More details can be found in Appendix.D from Gorishniy et al. (2024). When tuning TabR[‡] on the datasets from Table 5, we have used 25 tuning iterations and the same tuning space as for TabR from Rubachev et al. (2024).

D.12 FT-TRANSFORMER

We used the implementation from the "rtdl_revisiting_models" Python package. The results on datasets from Table 5 were copied from Rubachev et al. (2024), because the experiment setups are compatible.

D.13 MODERNNCA

Feature embeddings. We adapted an official implementation of Ye et al. (2024). We have used periodic embeddings Gorishniy et al. (2022) (specifically, `PeriodicEmbeddings(lite=True)` from the `rtdl_num_embeddings` Python package) for ModernNCA[‡] and no embeddings for

Table 11: The hyperparameter tuning space for FT-Transformer [Gorishniy et al. \(2021\)](#). Here, (B) = {Coverttype, Microsoft} and (A) contains all other datasets (except [Table 5](#)).

Parameter	Distribution or Value
# blocks	UniformInt[1, 4]
d_{token}	UniformInt[16, 384]
Attention dropout rate	Uniform[0.0, 0.5]
FFN hidden dimension expansion rate	Uniform[2/3, 8/3]
FFN dropout rate	Uniform[0.0, 0.5]
Residual dropout rate	{0.0, Uniform[0.0, 0.2]}
Learning rate	LogUniform[3e-5, 1e-3]
Weight decay	{0, LogUniform[1e-4, 1e-1]}
# Tuning iterations	(A) 100 (B) 50

ModernNCA. [Table 12](#) and [Table 13](#) provides hyperparameter tuning spaces for each ModernNCA and ModernNCA[‡].

Table 12: The hyperparameter tuning space for ModernNCA. Here, (C) = {[Table 5](#)}, (B) = {Coverttype, Microsoft} and (A) contains all other datasets.

Parameter	Distribution
# blocks	UniformInt[0, 2]
d_{block}	UniformInt[64, 1024]
dim	UniformInt[64, 1024]
Dropout rate	Uniform[0.0, 0.5]
Sample rate	Uniform[0.05, 0.6]
Learning rate	LogUniform[1e-5, 1e-1]
Weight decay	{0, LogUniform[1e-6, 1e-3]}
# Tuning iterations	(A) 100 (B, C) 50

Table 13: The hyperparameter tuning space for ModernNCA[‡]. Here, (C) = {[Table 5](#)}, (B) = {Coverttype, Microsoft} and (A) contains all other datasets.

Parameter	Distribution
# blocks	UniformInt[0, 2]
d_{block}	UniformInt[64, 1024]
dim	UniformInt[64, 1024]
Dropout rate	Uniform[0.0, 0.5]
Sample rate	Uniform[0.05, 0.6]
Learning rate	LogUniform[1e-5, 1e-1]
Weight decay	{0, LogUniform[1e-6, 1e-3]}
n_frequencies	UniformInt[16, 96]
d_embedding	UniformInt[16, 32]
frequency_init_scale	LogUniform[0.01, 10]
# Tuning iterations	(A) 100 (B, C) 50

D.14 T2G-FORMER

We adapted the implementation and hyperparameters of Yan et al. (2023) from the official repository¹. Table 14 provides hyperparameter tuning space.

Table 14: The hyperparameter tuning space for T2G-Former Yan et al. (2023). Here, (C) = {Table 5}, (B) = {Coverttype, Microsoft} and (A) contains all other datasets. Also, we used 50 tuning iterations for some datasets from Grinsztajn et al. (2022).

Parameter	Distribution or Value
# blocks	(A) UniformInt[3, 4] (B, C) UniformInt[1, 3]
d_{token}	UniformInt[64, 512]
Attention dropout rate	Uniform[0.0, 0.5]
FFN hidden dimension expansion rate	(A, B) Uniform[$2/3$, $8/3$] (C) $4/3$
FFN dropout rate	Uniform[0.0, 0.5]
Residual dropout rate	{0.0, Uniform[0.0, 0.2]}
Learning rate	LogUniform[$3e-5$, $1e-3$]
Col. Learning rate	LogUniform[$5e-3$, $5e-2$]
Weight decay	{0, LogUniform[$1e-6$, $1e-1$]}
# Tuning iterations	(A) 100 (B) 50 (C) 25

D.15 SAINT

We completely adapted hyperparameters and protocol from Gorishniy et al. (2024) to evaluate SAINT on Grinsztajn et al. (2022) benchmark. Results on datasets from Table 4 were directly taken from Gorishniy et al. (2024). Additional details can be found in Appendix.D from Gorishniy et al. (2024). We have used a default configuration on big datasets due to very high cost of tuning (see Table 15).

Table 15: The default hyperparameters for SAINT (Somepalli et al., 2021) on datasets from Rubachev et al. (2024).

Parameter	Value
depth	2
d_{token}	32
n_{heads}	4
d_{head}	8
Attention dropout rate	0.1
FFN hidden dimension expansion rate	1
FFN dropout rate	0.8
Learning rate	$1e-4$
Weight decay	$1e-2$

D.16 EXCELFORMER

Feature embeddings. ExcelFormer (Chen et al., 2023a) uses custom non-linear feature embeddings based on a GLU-style activation, see the original paper for details.

¹<https://github.com/jyansir/t2g-former>

We adapted the implementation and hyperparameters of [Chen et al. \(2023a\)](#) from the official repository². For fair comparison with other models, we did not use the augmentation techniques from the paper in our experiments. See [Table 16](#).

Table 16: The hyperparameter tuning space for Excelformer [Chen et al. \(2023a\)](#). Here, (D) = {Homecredit, Maps Routing}, (C) = {[Table 5](#) w/o (D)}, (B) = {Covertypes, Microsoft} and (A) contains all other datasets.

Parameter	Distribution or Value
# blocks	(A, B) UniformInt[2, 5] (C) UniformInt[2, 4] (D) UniformInt[1, 3]
d_{token}	(A, B) {32, 64, 128, 256} (C) {16, 32, 64} (D) {4, 8, 16, 32}
n_{heads}	(A,B) {4, 8, 16, 32} (C) {4, 8, 16} (D) 4
Attention dropout rate	0.3
FFN dropout rate	0.0
Residual dropout rate	Uniform[0.0, 0.5]
Learning rate	LogUniform[3e-5, 1e-3]
Weight decay	{0, LogUniform[1e-4, 1e-1]}
# Tuning iterations	(A) 100 (B) 50 (C, D) 25

D.17 CATBOOST, XGBOOST AND LIGHTGBM

Since our setup is directly taken from [Gorishniy et al. \(2024\)](#), we simply reused their results for GBDTs from the official repository³. Importantly, in a series of preliminary experiments, we confirmed that those results are reproducible in our instance of their setup. The details can be found in Appendix.D from [Gorishniy et al. \(2024\)](#). Results on datasets from [Table 5](#) were copied from the paper ([Rubachev et al., 2024](#)).

D.18 AUTOINT

We used an implementation from [Gorishniy et al. \(2021\)](#) which is an adapted official implementation⁴.

Table 17: The hyperparameter tuning space for AutoInt ([Song et al., 2019](#)). Here, (B) = {Covertypes, Microsoft} and (A) contains all other datasets.

Parameter	Distribution
# blocks	UniformInt[1, 6]
d_{token}	UniformInt[8, 64]
n_{heads}	2
Attention dropout rate	{0, Uniform[0.0, 0.5]}
Embedding dropout rate	{0, Uniform[0.0, 0.5]}
Learning rate	LogUniform[3e-5, 1e-3]
Weight decay	{0, LogUniform[1e-4, 1e-1]}
# Tuning iterations	(A) 100 (B) 50

²<https://github.com/WhatAShot/ExcelFormer>

³<https://github.com/yandex-research/tabular-dl-tabr>

⁴<https://github.com/shichence/AutoInt>

D.18.1 TABPFN

Since TabPFN accepts only less than 10K training samples we use different subsamples of size 10K for different random seeds. Also, TabPFN is not applicable to regressions and datasets with more than 100 features.

E PER-DATASET RESULTS WITH STANDARD DEVIATIONS

Table 18: Extended results for the main benchmark. Results are grouped by datasets.

churn \uparrow			california \downarrow		
Method	Single model	Ensemble	Method	Single model	Ensemble
MLP	0.8553 ± 0.0029	0.8582 ± 0.0008	MLP	0.4948 ± 0.0058	0.4880 ± 0.0022
TabPFN	—	0.8624 ± 0.0008	TabPFN	—	—
ResNet	0.8545 ± 0.0044	0.8565 ± 0.0035	ResNet	0.4915 ± 0.0031	0.4862 ± 0.0017
DCN2	0.8567 ± 0.0020	0.8570 ± 0.0017	DCN2	0.4971 ± 0.0122	0.4779 ± 0.0022
SNN	0.8506 ± 0.0051	0.8533 ± 0.0033	SNN	0.5033 ± 0.0075	0.4933 ± 0.0035
Trompt	$0.8600 \pm nan$	—	Trompt	$0.4579 \pm nan$	—
AutoInt	0.8607 ± 0.0047	0.8622 ± 0.0003	AutoInt	0.4682 ± 0.0063	0.4490 ± 0.0028
MLP-Mixer	0.8592 ± 0.0036	0.8630 ± 0.0005	MLP-Mixer	0.4746 ± 0.0056	0.4509 ± 0.0029
Excel	0.8618 ± 0.0023	$0.8625 \pm nan$	Excel	0.4544 ± 0.0048	$0.4350 \pm nan$
SAINT	0.8603 ± 0.0029	—	SAINT	0.4680 ± 0.0048	—
FT-T	0.8593 ± 0.0028	0.8598 ± 0.0025	FT-T	0.4635 ± 0.0048	0.4515 ± 0.0016
T2G	0.8613 ± 0.0015	—	T2G	0.4640 ± 0.0100	$0.4462 \pm nan$
MLP [‡] -lite	0.8624 ± 0.0010	0.8638 ± 0.0012	MLP [‡] -lite	0.4652 ± 0.0045	0.4549 ± 0.0006
MLP [‡]	0.8624 ± 0.0026	0.8640 ± 0.0010	MLP [‡]	0.4597 ± 0.0058	0.4482 ± 0.0026
MLP [†]	0.8580 ± 0.0028	0.8605 ± 0.0018	MLP [†]	0.4530 ± 0.0029	0.4491 ± 0.0010
XGBoost	0.8605 ± 0.0022	0.8608 ± 0.0013	XGBoost	0.4327 ± 0.0016	0.4316 ± 0.0007
LightGBM	0.8600 ± 0.0008	0.8600 ± 0.0000	LightGBM	0.4352 ± 0.0019	0.4339 ± 0.0008
CatBoost	0.8582 ± 0.0017	0.8588 ± 0.0008	CatBoost	0.4294 ± 0.0012	0.4265 ± 0.0003
TabR	0.8599 ± 0.0025	0.8620 ± 0.0023	TabR	0.4030 ± 0.0023	0.3964 ± 0.0013
TabR [‡]	0.8625 ± 0.0021	—	TabR [‡]	0.3998 ± 0.0033	—
MNCA	0.8595 ± 0.0028	0.8615 ± 0.0013	MNCA	0.4239 ± 0.0012	0.4231 ± 0.0005
MNCA [‡]	0.8606 ± 0.0032	0.8607 ± 0.0008	MNCA [‡]	0.4142 ± 0.0031	0.4071 ± 0.0029
TabM	0.8613 ± 0.0025	0.8615 ± 0.0005	TabM	0.4509 ± 0.0032	0.4490 ± 0.0018
TabM[G]	0.8611 ± 0.0018	—	TabM[G]	0.4507 ± 0.0027	—
TabM _{mini}	0.8625 ± 0.0025	0.8638 ± 0.0021	TabM _{mini}	0.4476 ± 0.0036	0.4425 ± 0.0009
TabM _{mini} [†]	0.8608 ± 0.0019	0.8592 ± 0.0003	TabM _{mini} [†]	0.4314 ± 0.0036	0.4261 ± 0.0019

house ↓			adult ↑		
Method	Single model	Ensemble	Method	Single model	Ensemble
MLP	3.1117 ± 0.0294	3.0706 ± 0.0140	MLP	0.8540 ± 0.0018	0.8559 ± 0.0011
TabPFN	—	—	TabPFN	—	—
ResNet	3.1143 ± 0.0258	3.0706 ± 0.0098	ResNet	0.8554 ± 0.0011	0.8562 ± 0.0006
DCN2	3.3327 ± 0.0878	3.1303 ± 0.0410	DCN2	0.8582 ± 0.0011	0.8593 ± 0.0002
SNN	3.2176 ± 0.0376	3.1320 ± 0.0155	SNN	0.8582 ± 0.0009	0.8603 ± 0.0012
Trompt	$3.0638 \pm nan$	—	Trompt	$0.8590 \pm nan$	—
AutoInt	3.2157 ± 0.0436	3.1261 ± 0.0095	AutoInt	0.8592 ± 0.0016	0.8612 ± 0.0004
MLP-Mixer	3.1871 ± 0.0519	3.0184 ± 0.0086	MLP-Mixer	0.8598 ± 0.0013	0.8617 ± 0.0002
Excel	3.2460 ± 0.0685	$3.1097 \pm nan$	Excel	0.8613 ± 0.0024	$0.8641 \pm nan$
SAINT	3.2424 ± 0.0595	—	SAINT	0.8601 ± 0.0019	—
FT-T	3.1823 ± 0.0460	3.0974 ± 0.0334	FT-T	0.8588 ± 0.0015	0.8608 ± 0.0011
T2G	3.1613 ± 0.0320	$3.0982 \pm nan$	T2G	0.8601 ± 0.0011	$0.8622 \pm nan$
MLP ^{†-lite}	3.0633 ± 0.0248	3.0170 ± 0.0070	MLP ^{†-lite}	0.8693 ± 0.0007	0.8702 ± 0.0006
MLP [†]	3.0775 ± 0.0336	3.0268 ± 0.0170	MLP [†]	0.8694 ± 0.0011	0.8704 ± 0.0008
MLP [†]	3.0999 ± 0.0351	3.0401 ± 0.0071	MLP [†]	0.8603 ± 0.0009	0.8616 ± 0.0006
XGBoost	3.1773 ± 0.0102	3.1644 ± 0.0068	XGBoost	0.8720 ± 0.0006	0.8723 ± 0.0002
LightGBM	3.1774 ± 0.0087	3.1672 ± 0.0050	LightGBM	0.8713 ± 0.0007	0.8721 ± 0.0004
CatBoost	3.1172 ± 0.0125	3.1058 ± 0.0022	CatBoost	0.8714 ± 0.0012	0.8723 ± 0.0007
TabR	3.0667 ± 0.0403	2.9958 ± 0.0270	TabR	0.8646 ± 0.0022	0.8680 ± 0.0019
TabR [†]	3.1048 ± 0.0410	—	TabR [†]	0.8699 ± 0.0011	—
MNCA	3.0884 ± 0.0286	3.0538 ± 0.0072	MNCA	0.8677 ± 0.0018	0.8696 ± 0.0003
MNCA [†]	3.0704 ± 0.0388	3.0149 ± 0.0308	MNCA [†]	0.8717 ± 0.0008	0.8742 ± 0.0006
TabM	3.0002 ± 0.0182	2.9796 ± 0.0024	TabM	0.8582 ± 0.0011	0.8588 ± 0.0003
TabM[G]	3.0156 ± 0.0231	—	TabM[G]	0.8577 ± 0.0009	—
TabM _{mini}	3.0496 ± 0.0225	3.0225 ± 0.0077	TabM _{mini}	0.8584 ± 0.0010	0.8591 ± 0.0005
TabM _{mini} [†]	2.9902 ± 0.0271	2.9648 ± 0.0035	TabM _{mini} [†]	0.8679 ± 0.0017	0.8690 ± 0.0005

diamond ↓			otto ↑		
Method	Single model	Ensemble	Method	Single model	Ensemble
MLP	0.1404 ± 0.0012	0.1362 ± 0.0003	MLP	0.8175 ± 0.0022	0.8222 ± 0.0007
TabPFN	—	—	TabPFN	—	0.7408 ± 0.0028
ResNet	0.1396 ± 0.0029	0.1361 ± 0.0011	ResNet	0.8174 ± 0.0021	0.8198 ± 0.0006
DCN2	0.1420 ± 0.0032	0.1374 ± 0.0020	DCN2	0.8064 ± 0.0021	0.8208 ± 0.0023
SNN	0.1473 ± 0.0057	0.1424 ± 0.0008	SNN	0.8087 ± 0.0020	0.8156 ± 0.0013
Trompt	$0.1391 \pm nan$	—	Trompt	$0.8093 \pm nan$	—
AutoInt	0.1392 ± 0.0014	0.1361 ± 0.0004	AutoInt	0.8050 ± 0.0034	0.8111 ± 0.0020
MLP-Mixer	0.1400 ± 0.0025	0.1378 ± 0.0008	MLP-Mixer	0.8092 ± 0.0040	0.8136 ± 0.0010
Excel	0.1766 ± 0.0023	$0.1712 \pm nan$	Excel	0.8102 ± 0.0022	$0.8220 \pm nan$
SAINT	0.1369 ± 0.0019	—	SAINT	0.8119 ± 0.0018	—
FT-T	0.1376 ± 0.0013	0.1360 ± 0.0002	FT-T	0.8133 ± 0.0033	0.8221 ± 0.0013
T2G	0.1372 ± 0.0011	$0.1346 \pm nan$	T2G	0.8161 ± 0.0019	$0.8272 \pm nan$
MLP ^{†-lite}	0.1342 ± 0.0008	0.1325 ± 0.0004	MLP ^{†-lite}	0.8190 ± 0.0021	0.8271 ± 0.0015
MLP [†]	0.1337 ± 0.0010	0.1317 ± 0.0003	MLP [†]	0.8189 ± 0.0015	0.8253 ± 0.0000
MLP [†]	0.1323 ± 0.0010	0.1301 ± 0.0005	MLP [†]	0.8205 ± 0.0021	0.8290 ± 0.0006
XGBoost	0.1368 ± 0.0004	0.1363 ± 0.0001	XGBoost	0.8297 ± 0.0011	0.8316 ± 0.0008
LightGBM	0.1359 ± 0.0002	0.1358 ± 0.0001	LightGBM	0.8302 ± 0.0009	0.8316 ± 0.0013
CatBoost	0.1335 ± 0.0006	0.1327 ± 0.0004	CatBoost	0.8250 ± 0.0013	0.8268 ± 0.0002
TabR	0.1327 ± 0.0010	0.1311 ± 0.0005	TabR	0.8179 ± 0.0022	0.8236 ± 0.0009
TabR [†]	0.1333 ± 0.0013	—	TabR [†]	0.8246 ± 0.0018	—
MNCA	0.1370 ± 0.0018	0.1348 ± 0.0005	MNCA	0.8275 ± 0.0012	0.8313 ± 0.0006
MNCA [†]	0.1327 ± 0.0012	0.1315 ± 0.0006	MNCA [†]	0.8265 ± 0.0015	0.8304 ± 0.0006
TabM	0.1342 ± 0.0017	0.1327 ± 0.0004	TabM	0.8268 ± 0.0014	0.8300 ± 0.0007
TabM[G]	0.1340 ± 0.0014	—	TabM[G]	0.8204 ± 0.0025	—
TabM _{mini}	0.1367 ± 0.0015	0.1352 ± 0.0008	TabM _{mini}	0.8267 ± 0.0011	0.8298 ± 0.0008
TabM _{mini} [†]	0.1320 ± 0.0010	0.1307 ± 0.0005	TabM _{mini} [†]	0.8342 ± 0.0014	0.8365 ± 0.0005

higgs-small \uparrow			black-friday \downarrow		
Method	Single model	Ensemble	Method	Single model	Ensemble
MLP	0.7180 ± 0.0027	0.7192 ± 0.0005	MLP	0.6955 ± 0.0004	0.6942 ± 0.0002
TabPFN	—	0.6727 ± 0.0034	TabPFN	—	—
ResNet	0.7256 ± 0.0020	0.7307 ± 0.0001	ResNet	0.6929 ± 0.0008	0.6907 ± 0.0002
DCN2	0.7164 ± 0.0030	0.7237 ± 0.0011	DCN2	0.6968 ± 0.0013	0.6936 ± 0.0007
SNN	0.7142 ± 0.0024	0.7171 ± 0.0020	SNN	0.6996 ± 0.0013	0.6978 ± 0.0004
Trompt	$0.7262 \pm nan$	—	Trompt	$0.6983 \pm nan$	—
AutoInt	0.7240 ± 0.0028	0.7287 ± 0.0008	AutoInt	0.6994 ± 0.0082	0.6927 ± 0.0021
MLP-Mixer	0.7248 ± 0.0023	0.7334 ± 0.0007	MLP-Mixer	0.6905 ± 0.0021	0.6851 ± 0.0011
Excel	0.7262 ± 0.0017	$0.7329 \pm nan$	Excel	0.6947 ± 0.0016	$0.6908 \pm nan$
SAINT	0.7236 ± 0.0019	—	SAINT	0.6934 ± 0.0009	—
FT-T	0.7281 ± 0.0016	0.7334 ± 0.0013	FT-T	0.6987 ± 0.0192	0.6879 ± 0.0023
T2G	0.7352 ± 0.0037	$0.7400 \pm nan$	T2G	0.6887 ± 0.0046	$0.6832 \pm nan$
MLP ^{†-lite}	0.7260 ± 0.0017	0.7304 ± 0.0008	MLP ^{†-lite}	0.6849 ± 0.0006	0.6824 ± 0.0002
MLP [†]	0.7261 ± 0.0010	0.7270 ± 0.0003	MLP [†]	0.6857 ± 0.0004	0.6838 ± 0.0002
MLP [†]	0.7210 ± 0.0016	0.7252 ± 0.0005	MLP [†]	0.6836 ± 0.0006	0.6812 ± 0.0002
XGBoost	0.7246 ± 0.0015	0.7264 ± 0.0013	XGBoost	0.6806 ± 0.0001	0.6805 ± 0.0000
LightGBM	0.7256 ± 0.0009	0.7263 ± 0.0007	LightGBM	0.6799 ± 0.0003	0.6795 ± 0.0001
CatBoost	0.7260 ± 0.0011	0.7273 ± 0.0010	CatBoost	0.6822 ± 0.0003	0.6813 ± 0.0002
TabR	0.7223 ± 0.0010	0.7257 ± 0.0008	TabR	0.6899 ± 0.0004	0.6883 ± 0.0002
TabR [†]	0.7294 ± 0.0014	—	TabR [†]	0.6761 ± 0.0009	—
MNCA	0.7263 ± 0.0023	0.7292 ± 0.0006	MNCA	0.6893 ± 0.0004	0.6883 ± 0.0000
MNCA [†]	0.7300 ± 0.0020	0.7348 ± 0.0008	MNCA [†]	0.6885 ± 0.0007	0.6863 ± 0.0003
TabM	0.7383 ± 0.0028	0.7409 ± 0.0010	TabM	0.6875 ± 0.0015	0.6866 ± 0.0003
TabM[G]	0.7372 ± 0.0021	—	TabM[G]	0.6870 ± 0.0014	—
TabM _{mini}	0.7344 ± 0.0016	0.7366 ± 0.0012	TabM _{mini}	0.6865 ± 0.0016	0.6843 ± 0.0005
TabM _{mini} [†]	0.7348 ± 0.0017	0.7379 ± 0.0006	TabM _{mini} [†]	0.6807 ± 0.0013	0.6783 ± 0.0009

covtype2 \uparrow			microsoft \downarrow		
Method	Single model	Ensemble	Method	Single model	Ensemble
MLP	0.9630 ± 0.0012	0.9664 ± 0.0004	MLP	0.7475 ± 0.0003	0.7460 ± 0.0003
TabPFN	—	0.7606 ± 0.0022	TabPFN	—	—
ResNet	0.9638 ± 0.0005	0.9685 ± 0.0003	ResNet	0.7472 ± 0.0004	0.7452 ± 0.0004
DCN2	0.9622 ± 0.0019	0.9673 ± 0.0011	DCN2	0.7499 ± 0.0003	0.7477 ± 0.0001
SNN	0.9636 ± 0.0010	0.9677 ± 0.0002	SNN	0.7488 ± 0.0004	0.7470 ± 0.0001
Trompt	$0.9286 \pm nan$	—	Trompt	$0.7476 \pm nan$	—
AutoInt	0.9614 ± 0.0016	0.9696 ± 0.0005	AutoInt	0.7482 ± 0.0005	0.7455 ± 0.0002
MLP-Mixer	0.9663 ± 0.0019	0.9699 ± 0.0014	MLP-Mixer	0.7482 ± 0.0008	0.7436 ± 0.0001
Excel	0.9606 ± 0.0018	$0.9670 \pm nan$	Excel	0.7479 ± 0.0007	$0.7442 \pm nan$
SAINT	0.9669 ± 0.0010	—	SAINT	0.7625 ± 0.0066	—
FT-T	0.9698 ± 0.0008	0.9731 ± 0.0006	FT-T	0.7460 ± 0.0007	0.7422 ± 0.0004
T2G	0.9668 ± 0.0008	$0.9708 \pm nan$	T2G	0.7460 ± 0.0006	$0.7427 \pm nan$
MLP ^{†-lite}	0.9690 ± 0.0008	0.9721 ± 0.0006	MLP ^{†-lite}	0.7446 ± 0.0002	0.7434 ± 0.0002
MLP [†]	0.9713 ± 0.0006	0.9758 ± 0.0000	MLP [†]	0.7444 ± 0.0003	0.7429 ± 0.0001
MLP [†]	0.9697 ± 0.0008	0.9721 ± 0.0005	MLP [†]	0.7465 ± 0.0005	0.7448 ± 0.0001
XGBoost	0.9710 ± 0.0002	0.9713 ± 0.0000	XGBoost	0.7413 ± 0.0001	0.7410 ± 0.0000
LightGBM	0.9709 ± 0.0003	—	LightGBM	0.7417 ± 0.0001	0.7413 ± 0.0000
CatBoost	0.9670 ± 0.0003	0.9680 ± 0.0002	CatBoost	0.7412 ± 0.0001	0.7406 ± 0.0000
TabR	0.9737 ± 0.0005	0.9745 ± 0.0006	TabR	0.7503 ± 0.0006	0.7485 ± 0.0002
TabR [†]	0.9752 ± 0.0003	—	TabR [†]	0.7501 ± 0.0005	—
MNCA	0.9724 ± 0.0003	0.9729 ± 0.0001	MNCA	0.7458 ± 0.0003	0.7448 ± 0.0002
MNCA [†]	0.9747 ± 0.0002	0.9747 ± 0.0002	MNCA [†]	0.7460 ± 0.0008	0.7435 ± 0.0004
TabM	0.9712 ± 0.0008	0.9729 ± 0.0003	TabM	0.7434 ± 0.0003	0.7424 ± 0.0001
TabM[G]	0.9707 ± 0.0008	—	TabM[G]	0.7435 ± 0.0003	—
TabM _{mini}	0.9693 ± 0.0008	0.9713 ± 0.0001	TabM _{mini}	0.7444 ± 0.0003	0.7431 ± 0.0002
TabM _{mini} [†]	0.9740 ± 0.0006	0.9754 ± 0.0001	TabM _{mini} [†]	0.7427 ± 0.0002	0.7416 ± 0.0002

Table 19: Extended results for the main benchmark. Results are grouped by datasets.

wine \uparrow			phoneme \uparrow		
Method	Single model	Ensemble	Method	Single model	Ensemble
MLP	0.7778 ± 0.0153	0.7907 ± 0.0117	MLP	0.8525 ± 0.0126	0.8635 ± 0.0099
TabPFN	—	0.7908 ± 0.0063	TabPFN	—	0.8684 ± 0.0050
ResNet	0.7710 ± 0.0137	0.7839 ± 0.0083	ResNet	0.8456 ± 0.0121	0.8504 ± 0.0066
DCN2	0.7492 ± 0.0147	0.7764 ± 0.0095	DCN2	0.8342 ± 0.0151	0.8543 ± 0.0118
SNN	0.7818 ± 0.0143	0.7994 ± 0.0097	SNN	0.8596 ± 0.0124	0.8687 ± 0.0080
Trompt	0.7818 ± 0.0081	—	Trompt	0.8465 ± 0.0205	—
AutoInt	0.7745 ± 0.0144	0.7909 ± 0.0160	AutoInt	0.8623 ± 0.0138	0.8754 ± 0.0095
MLP-Mixer	0.7769 ± 0.0149	0.7950 ± 0.0087	MLP-Mixer	0.8629 ± 0.0123	0.8757 ± 0.0095
Excel	0.7631 ± 0.0171	0.7765 ± 0.0121	Excel	0.8551 ± 0.0092	0.8711 ± 0.0081
SAINT	0.7684 ± 0.0144	—	SAINT	0.8657 ± 0.0130	—
FT-T	0.7755 ± 0.0133	0.7894 ± 0.0083	FT-T	0.8667 ± 0.0127	0.8795 ± 0.0093
T2G	0.7733 ± 0.0118	0.7933 ± 0.0137	T2G	0.8672 ± 0.0166	0.8765 ± 0.0141
MLP [‡] -lite	0.7803 ± 0.0157	0.7964 ± 0.0146	MLP [‡] -lite	0.8742 ± 0.0120	0.8861 ± 0.0071
MLP [‡]	0.7733 ± 0.0185	0.7856 ± 0.0160	MLP [‡]	0.8757 ± 0.0118	0.8856 ± 0.0065
MLP [†]	0.7814 ± 0.0132	0.7919 ± 0.0098	MLP [†]	0.8647 ± 0.0098	0.8761 ± 0.0076
XGBoost	0.7949 ± 0.0178	0.8010 ± 0.0186	XGBoost	0.8682 ± 0.0174	0.8771 ± 0.0156
LightGBM	0.7890 ± 0.0160	0.7929 ± 0.0106	LightGBM	0.8702 ± 0.0129	0.8733 ± 0.0126
CatBoost	0.7994 ± 0.0131	0.8057 ± 0.0098	CatBoost	0.8827 ± 0.0117	0.8897 ± 0.0055
TabR	0.7936 ± 0.0114	0.8055 ± 0.0057	TabR	0.8781 ± 0.0096	0.8840 ± 0.0054
TabR [‡]	0.7804 ± 0.0148	—	TabR [‡]	0.8772 ± 0.0087	—
MNCA	0.7911 ± 0.0135	0.8005 ± 0.0121	MNCA	0.8835 ± 0.0079	0.8861 ± 0.0057
MNCA [‡]	0.7867 ± 0.0113	0.7953 ± 0.0114	MNCA [‡]	0.8828 ± 0.0082	0.8925 ± 0.0056
TabM	0.7961 ± 0.0136	0.8011 ± 0.0084	TabM	0.8701 ± 0.0167	0.8766 ± 0.0128
TabM[G]	0.7855 ± 0.0164	—	TabM[G]	0.8668 ± 0.0180	—
TabM _{mini}	0.7904 ± 0.0123	0.7986 ± 0.0055	TabM _{mini}	0.8686 ± 0.0153	0.8758 ± 0.0091
TabM _{mini} [†]	0.7886 ± 0.0167	0.7963 ± 0.0113	TabM _{mini} [†]	0.8790 ± 0.0098	0.8885 ± 0.0056

analcatsdata_supreme \downarrow			Mercedes-Benz_Greener_Manufacturing \downarrow		
Method	Single model	Ensemble	Method	Single model	Ensemble
MLP	0.0782 ± 0.0081	0.0766 ± 0.0090	MLP	8.3045 ± 0.8708	8.2682 ± 0.8992
TabPFN	—	—	TabPFN	—	—
ResNet	0.0852 ± 0.0076	0.0823 ± 0.0078	ResNet	8.4434 ± 0.7982	8.3178 ± 0.8482
DCN2	0.0811 ± 0.0137	0.0759 ± 0.0086	DCN2	8.3540 ± 0.8314	8.3021 ± 0.8579
SNN	0.0826 ± 0.0096	0.0779 ± 0.0098	SNN	8.2718 ± 0.8152	8.2236 ± 0.8479
Trompt	0.0782 ± 0.0095	—	Trompt	8.3409 ± 0.9840	—
AutoInt	0.0783 ± 0.0078	0.0768 ± 0.0083	AutoInt	8.4001 ± 0.9256	8.3237 ± 0.9658
MLP-Mixer	0.0770 ± 0.0082	0.0759 ± 0.0081	MLP-Mixer	8.2860 ± 0.8656	8.2398 ± 0.9023
Excel	0.0796 ± 0.0101	0.0776 ± 0.0101	Excel	8.2244 ± 0.8514	8.1918 ± 0.9387
SAINT	0.0773 ± 0.0078	—	SAINT	8.3556 ± 0.9566	—
FT-T	0.0787 ± 0.0086	0.0775 ± 0.0091	FT-T	8.2252 ± 0.8617	8.1616 ± 0.8834
T2G	0.0775 ± 0.0081	0.0763 ± 0.0084	T2G	8.2120 ± 0.8485	8.1654 ± 0.9339
MLP [‡] -lite	0.0798 ± 0.0088	0.0769 ± 0.0092	MLP [‡] -lite	8.3045 ± 0.8708	8.2682 ± 0.8992
MLP [‡]	0.0786 ± 0.0073	0.0720 ± 0.0053	MLP [‡]	8.3045 ± 0.8708	8.2682 ± 0.8992
MLP [†]	0.0774 ± 0.0064	0.0759 ± 0.0063	MLP [†]	8.3045 ± 0.8708	8.2682 ± 0.8992
XGBoost	0.0801 ± 0.0126	0.0774 ± 0.0107	XGBoost	8.2177 ± 0.8175	8.2092 ± 0.8458
LightGBM	0.0778 ± 0.0115	0.0767 ± 0.0110	LightGBM	8.2078 ± 0.8231	8.1618 ± 0.8566
CatBoost	0.0780 ± 0.0067	0.0734 ± 0.0022	CatBoost	8.1629 ± 0.8193	8.1554 ± 0.8439
TabR	0.0803 ± 0.0066	0.0759 ± 0.0046	TabR	8.3506 ± 0.8149	8.2694 ± 0.8399
TabR [‡]	0.0807 ± 0.0088	—	TabR [‡]	8.3187 ± 0.8186	—
MNCA	0.0809 ± 0.0072	0.0784 ± 0.0062	MNCA	8.2557 ± 0.8602	8.1771 ± 0.8710
MNCA [‡]	0.0825 ± 0.0090	0.0793 ± 0.0072	MNCA [‡]	8.2557 ± 0.8602	8.1771 ± 0.8710
TabM	0.0777 ± 0.0099	0.0769 ± 0.0105	TabM	8.2215 ± 0.8940	8.1995 ± 0.9130
TabM[G]	0.0783 ± 0.0103	—	TabM[G]	8.2206 ± 0.8827	—
TabM _{mini}	0.0769 ± 0.0091	0.0758 ± 0.0097	TabM _{mini}	8.2375 ± 0.8953	8.2161 ± 0.9253
TabM _{mini} [†]	0.0790 ± 0.0079	0.0770 ± 0.0086	TabM _{mini} [†]	8.2375 ± 0.8953	8.2161 ± 0.9253

KDDCup09_upselling \uparrow			kdd_ipums_la_97-small \uparrow		
Method	Single model	Ensemble	Method	Single model	Ensemble
MLP	0.7759 ± 0.0137	0.7806 ± 0.0125	MLP	0.8828 ± 0.0061	0.8845 ± 0.0055
TabPFN	—	—	TabPFN	—	0.8578 ± 0.0046
ResNet	0.7811 ± 0.0124	0.7861 ± 0.0109	ResNet	0.8823 ± 0.0070	0.8824 ± 0.0060
DCN2	0.7850 ± 0.0161	0.7884 ± 0.0135	DCN2	0.8770 ± 0.0072	0.8824 ± 0.0068
SNN	0.7884 ± 0.0122	0.7940 ± 0.0116	SNN	0.8722 ± 0.0093	0.8733 ± 0.0083
Trompt	0.7994 ± 0.0055	—	Trompt	0.8847 ± 0.0070	—
AutoInt	0.8004 ± 0.0075	0.8037 ± 0.0063	AutoInt	0.8808 ± 0.0083	0.8830 ± 0.0081
MLP-Mixer	0.7979 ± 0.0105	0.8010 ± 0.0094	MLP-Mixer	0.8762 ± 0.0100	0.8770 ± 0.0088
Excel	0.7903 ± 0.0074	0.7939 ± 0.0099	Excel	0.8803 ± 0.0054	0.8823 ± 0.0071
SAINT	0.7942 ± 0.0112	—	SAINT	0.8837 ± 0.0055	—
FT-T	0.7957 ± 0.0127	0.7960 ± 0.0139	FT-T	0.8795 ± 0.0077	0.8792 ± 0.0062
T2G	0.8037 ± 0.0100	0.7988 ± 0.0084	T2G	0.8833 ± 0.0054	0.8841 ± 0.0062
MLP [†] -lite	0.7962 ± 0.0093	0.7995 ± 0.0105	MLP [†] -lite	0.8765 ± 0.0108	0.8765 ± 0.0108
MLP [†]	0.8005 ± 0.0097	0.8032 ± 0.0117	MLP [†]	0.8816 ± 0.0057	0.8818 ± 0.0048
MLP [†]	0.7925 ± 0.0123	0.7963 ± 0.0089	MLP [†]	0.8757 ± 0.0101	0.8756 ± 0.0104
XGBoost	0.7930 ± 0.0108	0.7950 ± 0.0102	XGBoost	0.8825 ± 0.0089	0.8835 ± 0.0085
LightGBM	0.7932 ± 0.0119	0.7969 ± 0.0115	LightGBM	0.8792 ± 0.0075	0.8802 ± 0.0067
CatBoost	0.7992 ± 0.0117	0.8010 ± 0.0121	CatBoost	0.8793 ± 0.0088	0.8803 ± 0.0100
TabR	0.7838 ± 0.0136	0.7859 ± 0.0167	TabR	0.8798 ± 0.0081	0.8819 ± 0.0078
TabR [†]	0.7908 ± 0.0123	—	TabR [†]	0.8831 ± 0.0050	—
MNCA	0.7939 ± 0.0097	0.7989 ± 0.0115	MNCA	0.8819 ± 0.0054	0.8832 ± 0.0048
MNCA [†]	0.7960 ± 0.0131	0.8008 ± 0.0110	MNCA [†]	0.8837 ± 0.0062	0.8860 ± 0.0059
TabM	0.8002 ± 0.0103	0.8021 ± 0.0074	TabM	0.8845 ± 0.0063	0.8848 ± 0.0070
TabM[G]	0.7974 ± 0.0124	—	TabM[G]	0.8846 ± 0.0059	—
TabM _{mini}	0.7963 ± 0.0123	0.8018 ± 0.0076	TabM _{mini}	0.8827 ± 0.0054	0.8810 ± 0.0050
TabM _{mini} [†]	0.8031 ± 0.0133	0.8039 ± 0.0114	TabM _{mini} [†]	0.8775 ± 0.0094	0.8780 ± 0.0099

wine_quality \downarrow			isolet \downarrow		
Method	Single model	Ensemble	Method	Single model	Ensemble
MLP	0.6707 ± 0.0178	0.6530 ± 0.0152	MLP	2.2744 ± 0.2203	2.0018 ± 0.1111
TabPFN	—	—	TabPFN	—	—
ResNet	0.6687 ± 0.0166	0.6543 ± 0.0170	ResNet	2.2077 ± 0.2248	1.9206 ± 0.1478
DCN2	0.7010 ± 0.0171	0.6699 ± 0.0139	DCN2	2.2449 ± 0.1579	2.0176 ± 0.0770
SNN	0.6604 ± 0.0174	0.6245 ± 0.0140	SNN	2.4269 ± 0.2382	2.1142 ± 0.1262
Trompt	0.6605 ± 0.0153	—	Trompt	2.6219 ± 0.0315	—
AutoInt	0.6840 ± 0.0126	0.6478 ± 0.0146	AutoInt	2.6130 ± 0.1658	2.3308 ± 0.1088
MLP-Mixer	0.6672 ± 0.0263	0.6294 ± 0.0200	MLP-Mixer	2.3344 ± 0.2073	2.0915 ± 0.1159
Excel	0.6881 ± 0.0182	0.6664 ± 0.0179	Excel	2.8691 ± 0.0882	2.5989 ± 0.0664
SAINT	0.6797 ± 0.0161	—	SAINT	2.7696 ± 0.0200	—
FT-T	0.6787 ± 0.0149	0.6564 ± 0.0250	FT-T	2.4879 ± 0.2524	2.1501 ± 0.1506
T2G	0.6783 ± 0.0170	0.6570 ± 0.0273	T2G	2.2867 ± 0.2489	1.9179 ± 0.1530
MLP [†] -lite	0.6569 ± 0.0167	0.6328 ± 0.0155	MLP [†] -lite	2.2719 ± 0.1006	2.1026 ± 0.1088
MLP [†]	0.6532 ± 0.0133	0.6336 ± 0.0140	MLP [†]	2.1832 ± 0.1124	2.0775 ± 0.0805
MLP [†]	0.6721 ± 0.0180	0.6463 ± 0.0262	MLP [†]	2.0979 ± 0.1779	1.9283 ± 0.1334
XGBoost	0.6039 ± 0.0134	0.6025 ± 0.0139	XGBoost	2.7567 ± 0.0470	2.7294 ± 0.0366
LightGBM	0.6135 ± 0.0138	0.6122 ± 0.0144	LightGBM	2.7005 ± 0.0296	2.6903 ± 0.0290
CatBoost	0.6088 ± 0.0132	0.6060 ± 0.0137	CatBoost	2.8847 ± 0.0227	2.8574 ± 0.0148
TabR	0.6315 ± 0.0097	0.6197 ± 0.0096	TabR	1.9760 ± 0.1738	1.7627 ± 0.1520
TabR [†]	0.6412 ± 0.0105	—	TabR [†]	1.9919 ± 0.1813	—
MNCA	0.6154 ± 0.0083	0.6058 ± 0.0149	MNCA	1.7905 ± 0.1594	1.6205 ± 0.1676
MNCA [†]	0.6099 ± 0.0144	0.6028 ± 0.0157	MNCA [†]	1.8912 ± 0.1851	1.7147 ± 0.1348
TabM	0.6169 ± 0.0123	0.6131 ± 0.0126	TabM	1.8831 ± 0.1194	1.8578 ± 0.1088
TabM[G]	0.6225 ± 0.0114	—	TabM[G]	1.9549 ± 0.1319	—
TabM _{mini}	0.6193 ± 0.0130	0.6138 ± 0.0140	TabM _{mini}	1.9966 ± 0.0923	1.9311 ± 0.0862
TabM _{mini} [†]	0.6255 ± 0.0146	0.6194 ± 0.0150	TabM _{mini} [†]	1.8378 ± 0.0803	1.8126 ± 0.0692

cpu_act ↓			bank-marketing ↑		
Method	Single model	Ensemble	Method	Single model	Ensemble
MLP	2.6814 ± 0.2291	2.4953 ± 0.1150	MLP	0.7860 ± 0.0057	0.7887 ± 0.0052
TabPFN	—	—	TabPFN	—	0.7894 ± 0.0091
ResNet	2.3933 ± 0.0641	2.3005 ± 0.0397	ResNet	0.7921 ± 0.0076	0.7932 ± 0.0066
DCN2	2.7868 ± 0.1999	2.4884 ± 0.0327	DCN2	0.7859 ± 0.0068	0.7917 ± 0.0078
SNN	2.5811 ± 0.1480	2.3863 ± 0.0324	SNN	0.7836 ± 0.0074	0.7882 ± 0.0054
Trompt	2.2133 ± 0.0221	—	Trompt	0.7975 ± 0.0080	—
AutoInt	2.2537 ± 0.0536	2.1708 ± 0.0349	AutoInt	0.7917 ± 0.0071	0.7956 ± 0.0058
MLP-Mixer	2.3079 ± 0.0829	2.1831 ± 0.0470	MLP-Mixer	0.7954 ± 0.0059	0.8001 ± 0.0048
Excel	2.3094 ± 0.2401	2.1411 ± 0.0767	Excel	0.7957 ± 0.0090	0.7985 ± 0.0106
SAINT	2.2781 ± 0.0630	—	SAINT	0.7953 ± 0.0058	—
FT-T	2.2394 ± 0.0508	2.1494 ± 0.0268	FT-T	0.7918 ± 0.0076	0.7951 ± 0.0071
T2G	2.2111 ± 0.0413	2.1330 ± 0.0316	T2G	0.7918 ± 0.0058	0.7955 ± 0.0047
MLP [‡] -lite	2.2730 ± 0.0457	2.1899 ± 0.0419	MLP [‡] -lite	0.7947 ± 0.0101	0.7977 ± 0.0117
MLP [‡]	2.2671 ± 0.0383	2.1940 ± 0.0433	MLP [‡]	0.7988 ± 0.0092	0.8024 ± 0.0093
MLP [†]	2.3309 ± 0.0719	2.2516 ± 0.0574	MLP [†]	0.7981 ± 0.0065	0.8008 ± 0.0057
XGBoost	2.5237 ± 0.3530	2.4723 ± 0.3789	XGBoost	0.8013 ± 0.0081	0.8030 ± 0.0076
LightGBM	2.2223 ± 0.0894	2.2067 ± 0.0916	LightGBM	0.8006 ± 0.0078	0.8013 ± 0.0072
CatBoost	2.1239 ± 0.0489	2.1092 ± 0.0499	CatBoost	0.8026 ± 0.0068	0.8056 ± 0.0082
TabR	2.2980 ± 0.0529	2.2228 ± 0.0501	TabR	0.7995 ± 0.0054	0.8015 ± 0.0037
TabR [‡]	2.1278 ± 0.0783	—	TabR [‡]	0.8023 ± 0.0088	—
MNCA	2.2603 ± 0.0479	2.2339 ± 0.0508	MNCA	0.7961 ± 0.0065	0.8003 ± 0.0077
MNCA [‡]	2.2105 ± 0.0483	2.1396 ± 0.0474	MNCA [‡]	0.7977 ± 0.0081	0.8010 ± 0.0084
TabM	2.1940 ± 0.0523	2.1677 ± 0.0487	TabM	0.7908 ± 0.0068	0.7915 ± 0.0068
TabM[G]	2.2033 ± 0.0552	—	TabM[G]	0.7902 ± 0.0067	—
TabM _{mini}	2.2254 ± 0.0734	2.1877 ± 0.0541	TabM _{mini}	0.7938 ± 0.0064	0.7959 ± 0.0071
TabM _{mini} [†]	2.1572 ± 0.0376	2.1222 ± 0.0358	TabM _{mini} [†]	0.8003 ± 0.0087	0.8017 ± 0.0087

Brazilian_houses ↓			MagicTelescope ↑		
Method	Single model	Ensemble	Method	Single model	Ensemble
MLP	0.0473 ± 0.0179	0.0440 ± 0.0207	MLP	0.8539 ± 0.0060	0.8566 ± 0.0061
TabPFN	—	—	TabPFN	—	0.8579 ± 0.0064
ResNet	0.0505 ± 0.0181	0.0458 ± 0.0207	ResNet	0.8589 ± 0.0068	0.8651 ± 0.0049
DCN2	0.0477 ± 0.0172	0.0427 ± 0.0207	DCN2	0.8432 ± 0.0074	0.8490 ± 0.0046
SNN	0.0630 ± 0.0162	0.0556 ± 0.0175	SNN	0.8536 ± 0.0052	0.8567 ± 0.0047
Trompt	0.0404 ± 0.0266	—	Trompt	0.8605 ± 0.0102	—
AutoInt	0.0470 ± 0.0192	0.0437 ± 0.0217	AutoInt	0.8522 ± 0.0056	0.8560 ± 0.0034
MLP-Mixer	0.0513 ± 0.0234	0.0484 ± 0.0262	MLP-Mixer	0.8571 ± 0.0080	0.8624 ± 0.0044
Excel	0.0450 ± 0.0156	0.0418 ± 0.0190	Excel	0.8480 ± 0.0090	0.8543 ± 0.0075
SAINT	0.0479 ± 0.0205	—	SAINT	0.8595 ± 0.0060	—
FT-T	0.0438 ± 0.0181	0.0412 ± 0.0204	FT-T	0.8588 ± 0.0046	0.8643 ± 0.0037
T2G	0.0468 ± 0.0165	0.0436 ± 0.0211	T2G	0.8553 ± 0.0055	0.8595 ± 0.0051
MLP [‡] -lite	0.0426 ± 0.0180	0.0397 ± 0.0206	MLP [‡] -lite	0.8591 ± 0.0061	0.8626 ± 0.0044
MLP [‡]	0.0437 ± 0.0203	0.0407 ± 0.0230	MLP [‡]	0.8575 ± 0.0056	0.8605 ± 0.0051
MLP [†]	0.0421 ± 0.0209	0.0409 ± 0.0226	MLP [†]	0.8593 ± 0.0054	0.8621 ± 0.0037
XGBoost	0.0541 ± 0.0270	0.0535 ± 0.0287	XGBoost	0.8550 ± 0.0094	0.8589 ± 0.0110
LightGBM	0.0603 ± 0.0249	0.0589 ± 0.0271	LightGBM	0.8547 ± 0.0085	0.8556 ± 0.0086
CatBoost	0.0468 ± 0.0312	0.0456 ± 0.0332	CatBoost	0.8586 ± 0.0070	0.8588 ± 0.0077
TabR	0.0490 ± 0.0152	0.0454 ± 0.0170	TabR	0.8682 ± 0.0058	0.8729 ± 0.0038
TabR [‡]	0.0451 ± 0.0163	—	TabR [‡]	0.8641 ± 0.0052	—
MNCA	0.0527 ± 0.0157	0.0509 ± 0.0180	MNCA	0.8602 ± 0.0061	0.8628 ± 0.0041
MNCA [‡]	0.0553 ± 0.0192	0.0511 ± 0.0191	MNCA [‡]	0.8622 ± 0.0085	0.8681 ± 0.0064
TabM	0.0443 ± 0.0213	0.0431 ± 0.0233	TabM	0.8607 ± 0.0058	0.8622 ± 0.0050
TabM[G]	0.0450 ± 0.0202	—	TabM[G]	0.8585 ± 0.0057	—
TabM _{mini}	0.0480 ± 0.0194	0.0452 ± 0.0221	TabM _{mini}	0.8581 ± 0.0053	0.8597 ± 0.0055
TabM _{mini} [†]	0.0460 ± 0.0206	0.0439 ± 0.0228	TabM _{mini} [†]	0.8616 ± 0.0080	0.8646 ± 0.0075

Ailerons ↓			MiamiHousing2016 ↓		
Method	Single model	Ensemble	Method	Single model	Ensemble
MLP	0.0002 ± 0.0000	0.0002 ± 0.0000	MLP	0.1614 ± 0.0033	0.1574 ± 0.0043
TabPFN	—	—	TabPFN	—	—
ResNet	0.0002 ± 0.0000	0.0002 ± 0.0000	ResNet	0.1548 ± 0.0030	0.1511 ± 0.0027
DCN2	0.0002 ± 0.0000	0.0002 ± 0.0000	DCN2	0.1683 ± 0.0099	0.1575 ± 0.0047
SNN	0.0002 ± 0.0000	0.0002 ± 0.0000	SNN	0.1618 ± 0.0029	0.1557 ± 0.0021
Trompt	0.0002 ± 0.0000	—	Trompt	0.1478 ± 0.0028	—
AutoInt	0.0002 ± 0.0000	0.0002 ± 0.0000	AutoInt	0.1537 ± 0.0035	0.1478 ± 0.0027
MLP-Mixer	0.0002 ± 0.0000	0.0002 ± 0.0000	MLP-Mixer	0.1527 ± 0.0037	0.1479 ± 0.0033
Excel	0.0002 ± 0.0000	0.0002 ± 0.0000	Excel	0.1519 ± 0.0038	0.1442 ± 0.0022
SAINT	0.0002 ± 0.0000	—	SAINT	0.1507 ± 0.0022	—
FT-T	0.0002 ± 0.0000	0.0002 ± 0.0000	FT-T	0.1514 ± 0.0029	0.1462 ± 0.0031
T2G	0.0002 ± 0.0000	0.0002 ± 0.0000	T2G	0.1523 ± 0.0023	0.1478 ± 0.0024
MLP [‡] -lite	0.0002 ± 0.0000	0.0002 ± 0.0000	MLP [‡] -lite	0.1514 ± 0.0025	0.1479 ± 0.0017
MLP [‡]	0.0002 ± 0.0000	0.0002 ± 0.0000	MLP [‡]	0.1512 ± 0.0019	0.1470 ± 0.0024
MLP [†]	0.0002 ± 0.0000	0.0002 ± 0.0000	MLP [†]	0.1461 ± 0.0015	0.1433 ± 0.0022
XGBoost	0.0002 ± 0.0000	0.0002 ± 0.0000	XGBoost	0.1440 ± 0.0029	0.1434 ± 0.0029
LightGBM	0.0002 ± 0.0000	0.0002 ± 0.0000	LightGBM	0.1461 ± 0.0025	0.1455 ± 0.0030
CatBoost	0.0002 ± 0.0000	0.0002 ± 0.0000	CatBoost	0.1417 ± 0.0021	0.1408 ± 0.0026
TabR	0.0002 ± 0.0000	0.0002 ± 0.0000	TabR	0.1417 ± 0.0025	0.1390 ± 0.0020
TabR [‡]	0.0002 ± 0.0000	—	TabR [‡]	0.1392 ± 0.0023	—
MNCA	0.0002 ± 0.0000	0.0002 ± 0.0000	MNCA	0.1503 ± 0.0040	0.1477 ± 0.0032
MNCA [‡]	0.0002 ± 0.0000	0.0002 ± 0.0000	MNCA [‡]	0.1475 ± 0.0031	0.1438 ± 0.0024
TabM	0.0002 ± 0.0000	0.0002 ± 0.0000	TabM	0.1483 ± 0.0030	0.1465 ± 0.0029
TabM[G]	0.0002 ± 0.0000	—	TabM[G]	0.1487 ± 0.0029	—
TabM _{mini}	0.0002 ± 0.0000	0.0002 ± 0.0000	TabM _{mini}	0.1508 ± 0.0035	0.1484 ± 0.0036
TabM _{mini} [†]	0.0002 ± 0.0000	0.0002 ± 0.0000	TabM _{mini} [†]	0.1407 ± 0.0016	0.1387 ± 0.0008

OnlineNewsPopularity ↓			credit ↑		
Method	Single model	Ensemble	Method	Single model	Ensemble
MLP	0.8643 ± 0.0007	0.8632 ± 0.0005	MLP	0.7735 ± 0.0042	0.7729 ± 0.0047
TabPFN	—	—	TabPFN	—	0.7636 ± 0.0045
ResNet	0.8665 ± 0.0011	0.8639 ± 0.0000	ResNet	0.7721 ± 0.0033	0.7738 ± 0.0027
DCN2	0.8714 ± 0.0013	0.8648 ± 0.0004	DCN2	0.7703 ± 0.0034	0.7746 ± 0.0026
SNN	0.8692 ± 0.0015	0.8665 ± 0.0005	SNN	0.7712 ± 0.0045	0.7716 ± 0.0059
Trompt	0.8623 ± <i>nan</i>	—	Trompt	0.7740 ± 0.0006	—
AutoInt	0.8636 ± 0.0022	0.8596 ± 0.0008	AutoInt	0.7737 ± 0.0050	0.7765 ± 0.0058
MLP-Mixer	0.8615 ± 0.0008	0.8598 ± 0.0004	MLP-Mixer	0.7748 ± 0.0038	0.7768 ± 0.0059
Excel	0.8605 ± 0.0024	0.8556 ± <i>nan</i>	Excel	0.7724 ± 0.0038	0.7740 ± 0.0069
SAINT	0.8600 ± 0.0007	—	SAINT	0.7739 ± 0.0052	—
FT-T	0.8629 ± 0.0019	0.8603 ± 0.0000	FT-T	0.7745 ± 0.0041	0.7767 ± 0.0040
T2G	0.8632 ± 0.0009	0.8572 ± <i>nan</i>	T2G	0.7744 ± 0.0046	0.7762 ± 0.0057
MLP [‡] -lite	0.8604 ± 0.0009	0.8591 ± 0.0004	MLP [‡] -lite	0.7749 ± 0.0055	0.7767 ± 0.0075
MLP [‡]	0.8594 ± 0.0004	0.8585 ± 0.0001	MLP [‡]	0.7734 ± 0.0034	0.7747 ± 0.0043
MLP [†]	0.8585 ± 0.0003	0.8581 ± 0.0001	MLP [†]	0.7758 ± 0.0040	0.7772 ± 0.0055
XGBoost	0.8545 ± 0.0002	0.8543 ± 0.0000	XGBoost	0.7698 ± 0.0027	0.7706 ± 0.0029
LightGBM	0.8546 ± 0.0002	0.8544 ± 0.0000	LightGBM	0.7686 ± 0.0028	0.7726 ± 0.0034
CatBoost	0.8532 ± 0.0003	0.8527 ± 0.0001	CatBoost	0.7734 ± 0.0035	0.7752 ± 0.0038
TabR	0.8677 ± 0.0013	0.8633 ± 0.0009	TabR	0.7730 ± 0.0043	0.7740 ± 0.0040
TabR [‡]	0.8624 ± 0.0011	—	TabR [‡]	0.7723 ± 0.0037	—
MNCA	0.8651 ± 0.0003	0.8650 ± 0.0002	MNCA	0.7739 ± 0.0032	0.7757 ± 0.0026
MNCA [‡]	0.8647 ± 0.0010	0.8624 ± 0.0006	MNCA [‡]	0.7734 ± 0.0045	0.7754 ± 0.0040
TabM	0.8584 ± 0.0003	0.8581 ± 0.0001	TabM	0.7751 ± 0.0042	0.7755 ± 0.0049
TabM[G]	0.8586 ± 0.0005	—	TabM[G]	0.7744 ± 0.0036	—
TabM _{mini}	0.8592 ± 0.0004	0.8588 ± 0.0001	TabM _{mini}	0.7747 ± 0.0039	0.7758 ± 0.0042
TabM _{mini} [†]	0.8560 ± 0.0015	0.8532 ± 0.0008	TabM _{mini} [†]	0.7748 ± 0.0026	0.7757 ± 0.0036

elevators ↓			fifa ↓		
Method	Single model	Ensemble	Method	Single model	Ensemble
MLP	0.0020 ± 0.0001	0.0019 ± 0.0000	MLP	0.8038 ± 0.0124	0.8011 ± 0.0143
TabPFN	—	—	TabPFN	—	—
ResNet	0.0019 ± 0.0000	0.0019 ± 0.0000	ResNet	0.8025 ± 0.0140	0.7985 ± 0.0149
DCN2	0.0019 ± 0.0000	0.0019 ± 0.0000	DCN2	0.8046 ± 0.0135	0.7993 ± 0.0129
SNN	0.0020 ± 0.0001	0.0019 ± 0.0000	SNN	0.8074 ± 0.0140	0.8031 ± 0.0147
Trompt	0.0018 ± 0.0000	—	Trompt	0.7880 ± 0.0180	—
AutoInt	0.0019 ± 0.0000	0.0018 ± 0.0000	AutoInt	0.7923 ± 0.0128	0.7886 ± 0.0127
MLP-Mixer	0.0019 ± 0.0000	0.0018 ± 0.0000	MLP-Mixer	0.7936 ± 0.0119	0.7903 ± 0.0133
Excel	0.0019 ± 0.0000	0.0018 ± 0.0000	Excel	0.7909 ± 0.0111	0.7862 ± 0.0161
SAINT	0.0018 ± 0.0000	—	SAINT	0.7901 ± 0.0118	—
FT-T	0.0019 ± 0.0000	0.0018 ± 0.0000	FT-T	0.7928 ± 0.0132	0.7888 ± 0.0130
T2G	0.0019 ± 0.0000	0.0018 ± 0.0000	T2G	0.7928 ± 0.0139	0.7904 ± 0.0183
MLP [‡] -lite	0.0019 ± 0.0000	0.0018 ± 0.0000	MLP [‡] -lite	0.7940 ± 0.0118	0.7898 ± 0.0141
MLP [‡]	0.0018 ± 0.0000	0.0018 ± 0.0000	MLP [‡]	0.7907 ± 0.0092	0.7870 ± 0.0096
MLP [†]	0.0018 ± 0.0000	0.0018 ± 0.0000	MLP [†]	0.7806 ± 0.0104	0.7800 ± 0.0114
XGBoost	0.0020 ± 0.0000	0.0020 ± 0.0000	XGBoost	0.7800 ± 0.0108	0.7795 ± 0.0114
LightGBM	0.0020 ± 0.0000	0.0020 ± 0.0000	LightGBM	0.7806 ± 0.0120	0.7787 ± 0.0122
CatBoost	0.0020 ± 0.0000	0.0019 ± 0.0000	CatBoost	0.7835 ± 0.0116	0.7817 ± 0.0114
TabR	0.0049 ± 0.0000	0.0049 ± 0.0000	TabR	0.7902 ± 0.0119	0.7863 ± 0.0120
TabR [‡]	0.0019 ± 0.0001	—	TabR [‡]	0.7914 ± 0.0136	—
MNCA	0.0019 ± 0.0000	0.0019 ± 0.0000	MNCA	0.7967 ± 0.0138	0.7933 ± 0.0145
MNCA [‡]	0.0018 ± 0.0000	0.0018 ± 0.0000	MNCA [‡]	0.7909 ± 0.0107	0.7866 ± 0.0106
TabM	0.0019 ± 0.0000	0.0018 ± 0.0000	TabM	0.7974 ± 0.0144	0.7954 ± 0.0160
TabM[G]	0.0019 ± 0.0000	—	TabM[G]	0.7970 ± 0.0146	—
TabM _{mini}	0.0019 ± 0.0000	0.0019 ± 0.0000	TabM _{mini}	0.7981 ± 0.0136	0.7947 ± 0.0154
TabM _{mini} [†]	0.0018 ± 0.0000	0.0018 ± 0.0000	TabM _{mini} [†]	0.7783 ± 0.0114	0.7768 ± 0.0123

house_sales ↓			medical_charges ↓		
Method	Single model	Ensemble	Method	Single model	Ensemble
MLP	0.1790 ± 0.0009	0.1763 ± 0.0003	MLP	0.0816 ± 0.0001	0.0814 ± 0.0000
TabPFN	—	—	TabPFN	—	—
ResNet	0.1755 ± 0.0014	0.1738 ± 0.0006	ResNet	0.0824 ± 0.0003	0.0817 ± 0.0001
DCN2	0.1862 ± 0.0032	0.1778 ± 0.0015	DCN2	0.0818 ± 0.0003	0.0815 ± 0.0001
SNN	0.1800 ± 0.0008	0.1770 ± 0.0004	SNN	0.0827 ± 0.0006	0.0817 ± 0.0001
Trompt	$0.1667 \pm nan$	—	Trompt	$0.0812 \pm nan$	—
AutoInt	0.1700 ± 0.0014	0.1670 ± 0.0008	AutoInt	0.0822 ± 0.0007	0.0814 ± 0.0001
MLP-Mixer	0.1704 ± 0.0007	0.1690 ± 0.0005	MLP-Mixer	0.0814 ± 0.0002	0.0811 ± 0.0000
Excel	0.1713 ± 0.0010	$0.1668 \pm nan$	Excel	0.0817 ± 0.0004	$0.0813 \pm nan$
SAINT	0.1713 ± 0.0015	—	SAINT	0.0814 ± 0.0002	—
FT-T	0.1690 ± 0.0010	0.1659 ± 0.0004	FT-T	0.0814 ± 0.0002	0.0812 ± 0.0000
T2G	0.1689 ± 0.0010	$0.1664 \pm nan$	T2G	0.0813 ± 0.0002	$0.0811 \pm nan$
MLP [‡] -lite	0.1699 ± 0.0008	0.1687 ± 0.0007	MLP [‡] -lite	0.0812 ± 0.0002	0.0810 ± 0.0000
MLP [‡]	0.1690 ± 0.0005	0.1676 ± 0.0003	MLP [‡]	0.0812 ± 0.0001	0.0809 ± 0.0001
MLP [†]	0.1687 ± 0.0004	0.1681 ± 0.0001	MLP [†]	0.0812 ± 0.0000	0.0811 ± 0.0000
XGBoost	0.1694 ± 0.0003	0.1689 ± 0.0001	XGBoost	0.0825 ± 0.0001	0.0825 ± 0.0000
LightGBM	0.1692 ± 0.0004	0.1686 ± 0.0001	LightGBM	0.0820 ± 0.0000	0.0820 ± 0.0000
CatBoost	0.1669 ± 0.0001	0.1667 ± 0.0000	CatBoost	0.0816 ± 0.0000	0.0815 ± 0.0000
TabR	0.1689 ± 0.0009	0.1657 ± 0.0003	TabR	0.0815 ± 0.0002	0.0812 ± 0.0000
TabR [‡]	0.1636 ± 0.0009	—	TabR [‡]	0.0811 ± 0.0001	—
MNCA	0.1737 ± 0.0013	0.1714 ± 0.0005	MNCA	0.0811 ± 0.0001	0.0810 ± 0.0000
MNCA [‡]	0.1694 ± 0.0007	0.1670 ± 0.0003	MNCA [‡]	0.0809 ± 0.0000	0.0808 ± 0.0000
TabM	0.1692 ± 0.0011	0.1680 ± 0.0005	TabM	0.0813 ± 0.0001	0.0812 ± 0.0000
TabM[G]	0.1692 ± 0.0009	—	TabM[G]	0.0812 ± 0.0000	—
TabM _{mini}	0.1687 ± 0.0009	0.1676 ± 0.0002	TabM _{mini}	0.0814 ± 0.0001	0.0813 ± 0.0000
TabM _{mini} [†]	0.1656 ± 0.0005	0.1647 ± 0.0002	TabM _{mini} [†]	0.0812 ± 0.0001	0.0812 ± 0.0000

pol ↓			superconduct ↓		
Method	Single model	Ensemble	Method	Single model	Ensemble
MLP	5.5244 ± 0.5768	4.9945 ± 0.5923	MLP	10.8740 ± 0.0868	10.4118 ± 0.0429
TabPFN	—	—	TabPFN	—	—
ResNet	6.3739 ± 0.6286	5.8181 ± 0.6054	ResNet	10.7711 ± 0.1454	10.3495 ± 0.0168
DCN2	6.5374 ± 0.9479	5.1814 ± 0.7775	DCN2	10.8108 ± 0.0957	10.4342 ± 0.0179
SNN	6.1816 ± 0.7366	5.5959 ± 0.8243	SNN	10.8562 ± 0.1300	10.3342 ± 0.0509
Trompt	3.2337 ± 0.0605	—	Trompt	10.4442 ± <i>nan</i>	—
AutoInt	3.3295 ± 0.3379	2.7999 ± 0.1776	AutoInt	11.0019 ± 0.1391	10.4469 ± 0.0521
MLP-Mixer	3.2011 ± 0.2921	2.8698 ± 0.2577	MLP-Mixer	10.7502 ± 0.0800	10.3281 ± 0.0450
Excel	3.0682 ± 0.2389	2.5816 ± 0.0368	Excel	11.0879 ± 0.1571	10.4094 ± <i>nan</i>
SAINT	2.7203 ± 0.1858	—	SAINT	10.7807 ± 0.1074	—
FT-T	2.6974 ± 0.1666	2.3718 ± 0.0724	FT-T	10.8256 ± 0.1692	10.3391 ± 0.0794
T2G	2.9539 ± 0.1994	2.6282 ± 0.0730	T2G	10.8310 ± 0.1406	10.3017 ± <i>nan</i>
MLP ^{†-lite}	2.8239 ± 0.2173	2.5266 ± 0.0605	MLP ^{†-lite}	10.5058 ± 0.0758	10.2322 ± 0.0463
MLP [†]	2.5452 ± 0.1221	2.3700 ± 0.0867	MLP [†]	10.5061 ± 0.0330	10.2440 ± 0.0127
MLP [†]	2.4958 ± 0.1292	2.3651 ± 0.1223	MLP [†]	10.7220 ± 0.0757	10.3758 ± 0.0606
XGBoost	4.2963 ± 0.0644	4.2548 ± 0.0488	XGBoost	10.1610 ± 0.0201	10.1413 ± 0.0025
LightGBM	4.2320 ± 0.3369	4.1880 ± 0.3110	LightGBM	10.1634 ± 0.0118	10.1552 ± 0.0050
CatBoost	3.6320 ± 0.1006	3.5505 ± 0.0896	CatBoost	10.2422 ± 0.0222	10.2116 ± 0.0058
TabR	6.0708 ± 0.5368	5.5578 ± 0.4036	TabR	10.8842 ± 0.1073	10.4800 ± 0.0280
TabR [†]	2.5770 ± 0.1689	—	TabR [†]	10.3835 ± 0.0562	—
MNCA	5.7878 ± 0.4884	5.3773 ± 0.5463	MNCA	10.4419 ± 0.0640	10.2926 ± 0.0261
MNCA [†]	2.9083 ± 0.1364	2.6717 ± 0.0530	MNCA [†]	10.5651 ± 0.0616	10.3155 ± 0.0253
TabM	3.3595 ± 0.4017	3.2130 ± 0.3979	TabM	10.3379 ± 0.0338	10.1943 ± 0.0291
TabM[G]	3.3465 ± 0.4226	—	TabM[G]	10.3395 ± 0.0529	—
TabM _{mini}	3.6925 ± 0.4469	3.4727 ± 0.3074	TabM _{mini}	10.3392 ± 0.0649	10.1866 ± 0.0400
TabM _{mini} [†]	2.4893 ± 0.1620	2.4175 ± 0.1124	TabM _{mini} [†]	10.2083 ± 0.0591	10.0737 ± 0.0222

jannis ↑			MiniBooNE ↑		
Method	Single model	Ensemble	Method	Single model	Ensemble
MLP	0.7840 ± 0.0018	0.7872 ± 0.0007	MLP	0.9480 ± 0.0007	0.9498 ± 0.0001
TabPFN	—	0.7419 ± 0.0018	TabPFN	—	0.9266 ± 0.0012
ResNet	0.7923 ± 0.0024	0.7958 ± 0.0010	ResNet	0.9488 ± 0.0011	0.9504 ± 0.0005
DCN2	0.7712 ± 0.0029	0.7825 ± 0.0009	DCN2	0.9433 ± 0.0011	0.9470 ± 0.0010
SNN	0.7818 ± 0.0025	0.7859 ± 0.0011	SNN	0.9476 ± 0.0013	0.9491 ± 0.0010
Trompt	0.8027 ± <i>nan</i>	—	Trompt	0.9473 ± <i>nan</i>	—
AutoInt	0.7933 ± 0.0018	0.7983 ± 0.0013	AutoInt	0.9447 ± 0.0014	0.9473 ± 0.0010
MLP-Mixer	0.7927 ± 0.0025	0.8019 ± 0.0012	MLP-Mixer	0.9446 ± 0.0014	0.9483 ± 0.0002
Excel	0.7954 ± 0.0015	0.8021 ± <i>nan</i>	Excel	0.9430 ± 0.0015	0.9451 ± <i>nan</i>
SAINT	0.7971 ± 0.0028	—	SAINT	0.9471 ± 0.0009	—
FT-T	0.7940 ± 0.0028	0.7998 ± 0.0006	FT-T	0.9467 ± 0.0014	0.9486 ± 0.0010
T2G	0.7998 ± 0.0024	0.8052 ± <i>nan</i>	T2G	0.9475 ± 0.0014	0.9508 ± <i>nan</i>
MLP ^{†-lite}	0.7923 ± 0.0018	0.7945 ± 0.0010	MLP ^{†-lite}	0.9466 ± 0.0009	0.9478 ± 0.0004
MLP [†]	0.7947 ± 0.0017	0.7967 ± 0.0011	MLP [†]	0.9473 ± 0.0010	0.9493 ± 0.0004
MLP [†]	0.7891 ± 0.0013	0.7900 ± 0.0006	MLP [†]	0.9482 ± 0.0008	0.9492 ± 0.0001
XGBoost	0.7967 ± 0.0019	0.7998 ± 0.0007	XGBoost	0.9436 ± 0.0006	0.9452 ± 0.0003
LightGBM	0.7956 ± 0.0017	0.7968 ± 0.0005	LightGBM	0.9422 ± 0.0009	0.9427 ± 0.0003
CatBoost	0.7985 ± 0.0018	0.8009 ± 0.0012	CatBoost	0.9453 ± 0.0008	0.9459 ± 0.0005
TabR	0.7983 ± 0.0022	0.8023 ± 0.0018	TabR	0.9487 ± 0.0008	0.9500 ± 0.0002
TabR [†]	0.8051 ± 0.0023	—	TabR [†]	0.9475 ± 0.0007	—
MNCA	0.7993 ± 0.0019	0.8042 ± 0.0013	MNCA	0.9488 ± 0.0010	0.9505 ± 0.0001
MNCA [†]	0.8068 ± 0.0021	0.8128 ± 0.0007	MNCA [†]	0.9493 ± 0.0012	0.9501 ± 0.0008
TabM	0.8066 ± 0.0015	0.8075 ± 0.0004	TabM	0.9500 ± 0.0005	0.9505 ± 0.0002
TabM[G]	0.8055 ± 0.0022	—	TabM[G]	0.9489 ± 0.0010	—
TabM _{mini}	0.8046 ± 0.0026	0.8062 ± 0.0011	TabM _{mini}	0.9487 ± 0.0006	0.9494 ± 0.0002
TabM _{mini} [†]	0.8059 ± 0.0018	0.8085 ± 0.0006	TabM _{mini} [†]	0.9497 ± 0.0006	0.9508 ± 0.0003

nyc-taxi-green-dec-2016 ↓			particulate-matter-ukair-2017 ↓		
Method	Single model	Ensemble	Method	Single model	Ensemble
MLP	0.3951 ± 0.0009	0.3921 ± 0.0003	MLP	0.3759 ± 0.0004	0.3729 ± 0.0003
TabPFN	—	—	TabPFN	—	—
ResNet	0.3899 ± 0.0016	0.3873 ± 0.0009	ResNet	0.3743 ± 0.0007	0.3718 ± 0.0005
DCN2	0.3919 ± 0.0009	0.3889 ± 0.0003	DCN2	0.3759 ± 0.0012	0.3738 ± 0.0004
SNN	0.3933 ± 0.0013	0.3899 ± 0.0004	SNN	0.3790 ± 0.0007	0.3744 ± 0.0002
Trompt	0.3979 ± <i>nan</i>	—	Trompt	0.3700 ± <i>nan</i>	—
AutoInt	0.4084 ± 0.0256	0.3967 ± 0.0059	AutoInt	0.3723 ± 0.0011	0.3692 ± 0.0010
MLP-Mixer	0.3914 ± 0.0026	0.3861 ± 0.0013	MLP-Mixer	0.3741 ± 0.0010	0.3698 ± 0.0004
Excel	0.3969 ± 0.0036	0.3897 ± <i>nan</i>	Excel	0.3699 ± 0.0014	0.3652 ± <i>nan</i>
SAINT	0.3905 ± 0.0013	—	SAINT	0.3704 ± 0.0014	—
FT-T	0.3937 ± 0.0064	0.3889 ± 0.0018	FT-T	0.3735 ± 0.0012	0.3686 ± 0.0004
T2G	0.3908 ± 0.0045	0.3858 ± <i>nan</i>	T2G	0.3676 ± 0.0024	0.3631 ± <i>nan</i>
MLP [‡] -lite	0.3812 ± 0.0018	0.3761 ± 0.0016	MLP [‡] -lite	0.3665 ± 0.0008	0.3642 ± 0.0003
MLP [‡]	0.3795 ± 0.0016	0.3733 ± 0.0013	MLP [‡]	0.3657 ± 0.0007	0.3629 ± 0.0002
MLP [†]	0.3680 ± 0.0006	0.3653 ± 0.0005	MLP [†]	0.3649 ± 0.0011	0.3637 ± 0.0008
XGBoost	0.3792 ± 0.0002	0.3787 ± 0.0000	XGBoost	0.3641 ± 0.0001	0.3640 ± 0.0000
LightGBM	0.3688 ± 0.0002	0.3684 ± 0.0000	LightGBM	0.3637 ± 0.0001	0.3635 ± 0.0000
CatBoost	0.3647 ± 0.0005	0.3632 ± 0.0003	CatBoost	0.3647 ± 0.0004	0.3637 ± 0.0002
TabR	0.3577 ± 0.0222	0.3380 ± 0.0027	TabR	0.3613 ± 0.0005	0.3590 ± 0.0002
TabR [‡]	0.3725 ± 0.0091	—	TabR [‡]	0.3596 ± 0.0004	—
MNCA	0.3728 ± 0.0012	0.3720 ± 0.0010	MNCA	0.3670 ± 0.0004	0.3649 ± 0.0002
MNCA [‡]	0.3536 ± 0.0052	0.3407 ± 0.0009	MNCA [‡]	0.3646 ± 0.0001	0.3643 ± 0.0000
TabM	0.3866 ± 0.0006	0.3855 ± 0.0003	TabM	0.3686 ± 0.0006	0.3679 ± 0.0003
TabM[G]	0.3862 ± 0.0005	—	TabM[G]	0.3683 ± 0.0007	—
TabM _{mini}	0.3877 ± 0.0009	0.3857 ± 0.0004	TabM _{mini}	0.3690 ± 0.0009	0.3675 ± 0.0004
TabM _{mini} [†]	0.3527 ± 0.0112	0.3478 ± 0.0009	TabM _{mini} [†]	0.3603 ± 0.0005	0.3589 ± 0.0003

road-safety ↑			year ↓		
Method	Single model	Ensemble	Method	Single model	Ensemble
MLP	0.7857 ± 0.0019	0.7873 ± 0.0004	MLP	8.9628 ± 0.0232	8.8931 ± 0.0066
TabPFN	—	0.7338 ± 0.0032	TabPFN	—	—
ResNet	0.7875 ± 0.0007	0.7898 ± 0.0008	ResNet	8.9658 ± 0.0239	8.8755 ± 0.0066
DCN2	0.7781 ± 0.0014	0.7823 ± 0.0012	DCN2	9.2761 ± 0.0401	9.0640 ± 0.0156
SNN	0.7847 ± 0.0010	0.7865 ± 0.0002	SNN	9.0054 ± 0.0256	8.9351 ± 0.0073
Trompt	0.7804 ± <i>nan</i>	—	Trompt	8.9707 ± <i>nan</i>	—
AutoInt	0.7826 ± 0.0030	0.7883 ± 0.0013	AutoInt	9.0430 ± 0.0280	8.9619 ± 0.0092
MLP-Mixer	0.7878 ± 0.0032	0.7919 ± 0.0015	MLP-Mixer	8.9589 ± 0.0182	8.9086 ± 0.0177
Excel	0.7864 ± 0.0053	0.7907 ± <i>nan</i>	Excel	9.0395 ± 0.0266	8.9551 ± <i>nan</i>
SAINT	0.7584 ± 0.0584	—	SAINT	9.0248 ± 0.0225	—
FT-T	0.7907 ± 0.0012	0.7943 ± 0.0007	FT-T	9.0005 ± 0.0215	8.9360 ± 0.0013
T2G	0.7912 ± 0.0026	0.7961 ± <i>nan</i>	T2G	8.9775 ± 0.0138	8.8979 ± <i>nan</i>
MLP [‡] -lite	0.7867 ± 0.0018	0.7903 ± 0.0002	MLP [‡] -lite	8.9355 ± 0.0103	8.9063 ± 0.0030
MLP [‡]	0.7853 ± 0.0014	0.7881 ± 0.0007	MLP [‡]	8.9455 ± 0.0173	8.9083 ± 0.0046
MLP [†]	0.7899 ± 0.0009	0.7935 ± 0.0003	MLP [†]	8.9379 ± 0.0206	8.8753 ± 0.0038
XGBoost	0.8101 ± 0.0017	0.8129 ± 0.0004	XGBoost	9.0307 ± 0.0028	9.0245 ± 0.0015
LightGBM	0.7982 ± 0.0012	0.7996 ± 0.0005	LightGBM	9.0200 ± 0.0025	9.0128 ± 0.0015
CatBoost	0.8012 ± 0.0009	0.8022 ± 0.0002	CatBoost	9.0370 ± 0.0073	9.0054 ± 0.0028
TabR	0.8403 ± 0.0014	0.8441 ± 0.0005	TabR	9.0069 ± 0.0152	8.9132 ± 0.0088
TabR [‡]	0.8374 ± 0.0013	—	TabR [‡]	8.9721 ± 0.0105	—
MNCA	0.8080 ± 0.0013	0.8121 ± 0.0006	MNCA	8.9476 ± 0.0152	8.8977 ± 0.0037
MNCA [‡]	0.8232 ± 0.0017	0.8287 ± 0.0008	MNCA [‡]	8.8973 ± 0.0082	8.8550 ± 0.0031
TabM	0.7946 ± 0.0013	0.7961 ± 0.0005	TabM	8.8701 ± 0.0110	8.8517 ± 0.0022
TabM[G]	0.7945 ± 0.0009	—	TabM[G]	8.8715 ± 0.0116	—
TabM _{mini}	0.7931 ± 0.0011	0.7946 ± 0.0010	TabM _{mini}	8.8958 ± 0.0087	8.8810 ± 0.0020
TabM _{mini} [†]	0.8015 ± 0.0034	0.8060 ± 0.0015	TabM _{mini} [†]	8.8825 ± 0.0087	8.8560 ± 0.0015

Table 20: Extended results for the main benchmark. Results are grouped by datasets.

sberbank-housing ↓			ecom-offers ↑		
Method	Single model	Ensemble	Method	Single model	Ensemble
MLP	0.2529 ± 0.0078	0.2474 ± 0.0052	MLP	0.5989 ± 0.0017	0.5995 ± 0.0011
TabPFN	—	—	TabPFN	—	—
ResNet	—	—	ResNet	—	—
DCN2	0.2616 ± 0.0049	0.2506 ± 0.0015	DCN2	0.5996 ± 0.0043	0.6039 ± 0.0028
SNN	0.2671 ± 0.0140	0.2555 ± 0.0033	SNN	0.5912 ± 0.0056	0.5961 ± 0.0033
Trompt	0.2509 ± <i>nan</i>	—	Trompt	0.5803 ± <i>nan</i>	—
AutoInt	—	—	AutoInt	—	—
MLP-Mixer	—	—	MLP-Mixer	—	—
Excel	0.2533 ± 0.0046	0.2485 ± <i>nan</i>	Excel	0.5759 ± 0.0066	0.5759 ± <i>nan</i>
SAINT	0.2467 ± 0.0019	—	SAINT	0.5812 ± 0.0098	—
FT-T	0.2440 ± 0.0038	0.2367 ± 0.0010	FT-T	0.5775 ± 0.0063	0.5817 ± 0.0021
T2G	0.2416 ± 0.0025	0.2343 ± <i>nan</i>	T2G	0.5791 ± 0.0056	0.5824 ± <i>nan</i>
MLP [‡] -lite	0.2528 ± 0.0055	0.2503 ± 0.0029	MLP [‡] -lite	0.5800 ± 0.0029	0.5819 ± 0.0011
MLP [‡]	0.2412 ± 0.0031	0.2355 ± 0.0006	MLP [‡]	0.5846 ± 0.0048	0.5872 ± 0.0018
MLP [†]	0.2383 ± 0.0032	0.2327 ± 0.0009	MLP [†]	0.5949 ± 0.0013	0.5953 ± 0.0006
XGBoost	0.2419 ± 0.0012	0.2416 ± 0.0007	XGBoost	0.5763 ± 0.0072	0.5917 ± 0.0035
LightGBM	0.2468 ± 0.0009	0.2467 ± 0.0002	LightGBM	0.5758 ± 0.0006	0.5758 ± 0.0003
CatBoost	0.2482 ± 0.0034	0.2473 ± 0.0016	CatBoost	0.5596 ± 0.0068	0.5067 ± 0.0011
TabR	0.2820 ± 0.0323	0.2603 ± 0.0048	TabR	0.5943 ± 0.0019	0.5977 ± 0.0009
TabR [‡]	0.2542 ± 0.0101	—	TabR [‡]	0.5762 ± 0.0052	—
MNCA	0.2593 ± 0.0053	0.2520 ± 0.0032	MNCA	0.5765 ± 0.0087	0.5820 ± 0.0047
MNCA [‡]	0.2448 ± 0.0039	0.2404 ± 0.0025	MNCA [‡]	0.5758 ± 0.0050	0.5796 ± 0.0009
TabM	0.2469 ± 0.0035	0.2440 ± 0.0026	TabM	0.5948 ± 0.0006	0.5952 ± 0.0004
TabM[G]	0.2480 ± 0.0049	—	TabM[G]	0.5959 ± 0.0010	—
TabM _{mini}	0.2440 ± 0.0025	0.2425 ± 0.0008	TabM _{mini}	0.5948 ± 0.0009	0.5954 ± 0.0004
TabM _{mini} [†]	0.2357 ± 0.0025	0.2333 ± 0.0007	TabM _{mini} [†]	0.5919 ± 0.0016	0.5926 ± 0.0006

maps-routing ↓			homesite-insurance ↑		
Method	Single model	Ensemble	Method	Single model	Ensemble
MLP	0.1625 ± 0.0001	0.1621 ± 0.0000	MLP	0.9506 ± 0.0005	0.9514 ± 0.0001
TabPFN	—	—	TabPFN	—	—
ResNet	—	—	ResNet	—	—
DCN2	0.1656 ± 0.0004	0.1636 ± 0.0001	DCN2	0.9398 ± 0.0053	0.9432 ± 0.0018
SNN	0.1634 ± 0.0002	0.1625 ± 0.0000	SNN	0.9473 ± 0.0013	0.9484 ± 0.0007
Trompt	0.1624 ± <i>nan</i>	—	Trompt	0.9588 ± <i>nan</i>	—
AutoInt	—	—	AutoInt	—	—
MLP-Mixer	—	—	MLP-Mixer	—	—
Excel	0.1628 ± 0.0001	0.1621 ± <i>nan</i>	Excel	0.9622 ± 0.0004	0.9635 ± <i>nan</i>
SAINT	0.1634 ± <i>nan</i>	—	SAINT	0.9613 ± <i>nan</i>	—
FT-T	0.1625 ± 0.0003	0.1619 ± 0.0001	FT-T	0.9622 ± 0.0006	0.9633 ± 0.0001
T2G	0.1616 ± 0.0001	0.1608 ± <i>nan</i>	T2G	0.9624 ± 0.0006	0.9637 ± <i>nan</i>
MLP [‡] -lite	0.1618 ± 0.0002	0.1613 ± 0.0000	MLP [‡] -lite	0.9609 ± 0.0009	0.9626 ± 0.0003
MLP [‡]	0.1618 ± 0.0002	0.1613 ± 0.0001	MLP [‡]	0.9617 ± 0.0004	0.9630 ± 0.0002
MLP [†]	0.1620 ± 0.0002	0.1614 ± 0.0000	MLP [†]	0.9582 ± 0.0014	0.9599 ± 0.0002
XGBoost	0.1616 ± 0.0001	0.1614 ± 0.0000	XGBoost	0.9601 ± 0.0002	0.9602 ± 0.0000
LightGBM	0.1618 ± 0.0000	0.1616 ± 0.0000	LightGBM	0.9603 ± 0.0002	0.9604 ± 0.0001
CatBoost	0.1619 ± 0.0001	0.1615 ± 0.0000	CatBoost	0.9606 ± 0.0003	0.9609 ± 0.0001
TabR	0.1639 ± 0.0003	0.1622 ± 0.0002	TabR	0.9487 ± 0.0014	0.9505 ± 0.0001
TabR [‡]	0.1622 ± 0.0002	—	TabR [‡]	0.9556 ± 0.0021	—
MNCA	0.1625 ± 0.0001	0.1621 ± 0.0001	MNCA	0.9514 ± 0.0038	0.9522 ± 0.0027
MNCA [‡]	0.1627 ± 0.0002	0.1623 ± 0.0001	MNCA [‡]	0.9620 ± 0.0006	0.9635 ± 0.0002
TabM	0.1612 ± 0.0001	0.1609 ± 0.0000	TabM	0.9641 ± 0.0004	0.9644 ± 0.0003
TabM[G]	0.1612 ± 0.0001	—	TabM[G]	0.9640 ± 0.0004	—
TabM _{mini}	0.1613 ± 0.0002	0.1609 ± 0.0000	TabM _{mini}	0.9642 ± 0.0003	0.9644 ± 0.0001
TabM _{mini} [†]	0.1610 ± 0.0001	0.1607 ± 0.0001	TabM _{mini} [†]	0.9627 ± 0.0002	0.9630 ± 0.0001

cooking-time ↓			homecredit-default ↑		
Method	Single model	Ensemble	Method	Single model	Ensemble
MLP	0.4828 ± 0.0002	0.4822 ± 0.0000	MLP	0.8538 ± 0.0014	0.8566 ± 0.0005
TabPFN	—	—	TabPFN	—	—
ResNet	—	—	ResNet	—	—
DCN2	0.4834 ± 0.0003	0.4822 ± 0.0001	DCN2	0.8471 ± 0.0019	0.8549 ± 0.0002
SNN	0.4835 ± 0.0006	0.4818 ± 0.0002	SNN	0.8541 ± 0.0016	0.8569 ± 0.0010
Trompt	$0.4809 \pm nan$	—	Trompt	$0.8355 \pm nan$	—
AutoInt	—	—	AutoInt	—	—
MLP-Mixer	—	—	MLP-Mixer	—	—
Excel	0.4821 ± 0.0005	$0.4808 \pm nan$	Excel	0.8513 ± 0.0024	$0.8564 \pm nan$
SAINT	$0.4840 \pm nan$	—	SAINT	$0.8377 \pm nan$	—
FT-T	0.4820 ± 0.0008	0.4813 ± 0.0005	FT-T	0.8571 ± 0.0023	0.8611 ± 0.0013
T2G	0.4809 ± 0.0008	$0.4797 \pm nan$	T2G	0.8597 ± 0.0007	$0.8629 \pm nan$
MLP ^{†-lite}	0.4811 ± 0.0004	0.4805 ± 0.0001	MLP ^{†-lite}	0.8598 ± 0.0009	0.8607 ± 0.0003
MLP [†]	0.4809 ± 0.0006	0.4804 ± 0.0003	MLP [†]	0.8572 ± 0.0011	0.8590 ± 0.0003
MLP [†]	0.4812 ± 0.0004	0.4807 ± 0.0002	MLP [†]	0.8568 ± 0.0039	0.8614 ± 0.0014
XGBoost	0.4823 ± 0.0001	0.4821 ± 0.0000	XGBoost	0.8670 ± 0.0005	0.8674 ± 0.0001
LightGBM	0.4826 ± 0.0001	0.4825 ± 0.0001	LightGBM	0.8664 ± 0.0004	0.8667 ± 0.0000
CatBoost	0.4823 ± 0.0001	0.4820 ± 0.0001	CatBoost	$0.8627 \pm nan$	—
TabR	0.4828 ± 0.0008	0.4814 ± 0.0004	TabR	0.8501 ± 0.0027	0.8548 ± 0.0003
TabR [†]	0.4818 ± 0.0006	—	TabR [†]	0.8547 ± 0.0021	—
MNCA	0.4825 ± 0.0004	0.4819 ± 0.0003	MNCA	0.8531 ± 0.0018	0.8569 ± 0.0004
MNCA [†]	0.4818 ± 0.0005	0.4809 ± 0.0003	MNCA [†]	0.8544 ± 0.0033	0.8606 ± 0.0024
TabM	0.4803 ± 0.0006	0.4797 ± 0.0003	TabM	0.8583 ± 0.0010	0.8599 ± 0.0006
TabM[G]	0.4803 ± 0.0005	—	TabM[G]	0.8583 ± 0.0011	—
TabM _{mini}	0.4804 ± 0.0006	0.4796 ± 0.0000	TabM _{mini}	0.8577 ± 0.0017	0.8598 ± 0.0004
TabM _{mini} [†]	0.4805 ± 0.0007	0.4795 ± 0.0003	TabM _{mini} [†]	0.8632 ± 0.0017	0.8656 ± 0.0003

delivery-eta ↓			weather ↓		
Method	Single model	Ensemble	Method	Single model	Ensemble
MLP	0.5493 ± 0.0007	0.5478 ± 0.0006	MLP	1.5378 ± 0.0054	1.5111 ± 0.0029
TabPFN	—	—	TabPFN	—	—
ResNet	—	—	ResNet	—	—
DCN2	0.5516 ± 0.0014	0.5495 ± 0.0004	DCN2	1.5606 ± 0.0057	1.5292 ± 0.0028
SNN	0.5495 ± 0.0008	0.5479 ± 0.0001	SNN	1.5280 ± 0.0085	1.5013 ± 0.0034
Trompt	$0.5519 \pm nan$	—	Trompt	$1.5187 \pm nan$	—
AutoInt	—	—	AutoInt	—	—
MLP-Mixer	—	—	MLP-Mixer	—	—
Excel	0.5552 ± 0.0030	$0.5524 \pm nan$	Excel	1.5131 ± 0.0022	$1.4707 \pm nan$
SAINT	$0.5528 \pm nan$	—	SAINT	1.5097 ± 0.0045	—
FT-T	0.5542 ± 0.0026	0.5523 ± 0.0018	FT-T	1.5104 ± 0.0097	1.4719 ± 0.0040
T2G	0.5527 ± 0.0016	$0.5512 \pm nan$	T2G	1.4849 ± 0.0087	$1.4513 \pm nan$
MLP ^{†-lite}	0.5521 ± 0.0014	0.5512 ± 0.0005	MLP ^{†-lite}	1.5170 ± 0.0040	1.4953 ± 0.0023
MLP [†]	0.5535 ± 0.0019	0.5526 ± 0.0009	MLP [†]	1.5139 ± 0.0031	1.4978 ± 0.0020
MLP [†]	0.5521 ± 0.0019	0.5511 ± 0.0007	MLP [†]	1.5162 ± 0.0020	1.5066 ± 0.0008
XGBoost	0.5468 ± 0.0002	0.5463 ± 0.0001	XGBoost	1.4671 ± 0.0006	1.4629 ± 0.0002
LightGBM	0.5468 ± 0.0001	0.5465 ± 0.0000	LightGBM	1.4625 ± 0.0008	1.4581 ± 0.0003
CatBoost	0.5465 ± 0.0001	0.5461 ± 0.0000	CatBoost	1.4688 ± 0.0019	—
TabR	0.5514 ± 0.0024	0.5480 ± 0.0005	TabR	1.4666 ± 0.0039	1.4547 ± 0.0008
TabR [†]	0.5520 ± 0.0015	—	TabR [†]	1.4458 ± 0.0018	—
MNCA	0.5498 ± 0.0007	0.5488 ± 0.0002	MNCA	1.5062 ± 0.0054	1.4822 ± 0.0013
MNCA [†]	0.5507 ± 0.0013	0.5494 ± 0.0006	MNCA [†]	1.5008 ± 0.0034	1.4782 ± 0.0011
TabM	0.5510 ± 0.0015	0.5504 ± 0.0004	TabM	1.4786 ± 0.0039	1.4715 ± 0.0020
TabM[G]	0.5517 ± 0.0016	—	TabM[G]	1.4796 ± 0.0037	—
TabM _{mini}	0.5519 ± 0.0015	0.5511 ± 0.0006	TabM _{mini}	1.4809 ± 0.0027	1.4717 ± 0.0012
TabM _{mini} [†]	0.5508 ± 0.0013	0.5497 ± 0.0003	TabM _{mini} [†]	1.4709 ± 0.0047	1.4611 ± 0.0023